Prepared for submission to JHEP

Lattice potentials and fermions in holographic non Fermi-liquids: hybridizing local quantum criticality

Yan Liu, Koenraad Schalm, Ya-Wen Sun, and Jan Zaanen

Institute Lorentz for Theoretical Physics, Leiden University
P.O. Box 9506, Leiden 2300RA, The Netherlands

E-mail: liu, kschalm, sun, jan@lorentz.leidenuniv.nl.

Abstract: We study lattice effects in strongly coupled systems of fermions at a finite density described by a holographic dual consisting of fermions in Anti-de-Sitter space in the presence of a Reissner-Nordström black hole. The lattice effect is encoded by a periodic modulation of the chemical potential with a wavelength of order of the intrinsic length scales of the system. This corresponds with a highly complicated "band structure" problem in AdS, which we only manage to solve in the weak potential limit. The "domain wall" fermions in AdS encoding for the Fermi surfaces in the boundary field theory diffract as usually against the periodic lattice, giving rise to band gaps. However, the deep infrared of the field theory as encoded by the near horizon AdS_2 geometry in the bulk reacts in a surprising way to the weak potential. The hybridization of the fermions bulk dualizes into a linear combination of CFT_1 "local quantum critical" propagators in the bulk, characterized by momentum dependent exponents displaced by lattice Umklapp vectors. This has the consequence that the metals showing quasi-Fermi surfaces cannot be localized in band insulators. In the AdS_2 metal regime, where the conformal dimension of the fermionic operator is large and no Fermi surfaces are present at low T/μ, the lattice gives rise to a characteristic dependence of the energy scaling as a function of momentum. We predict crossovers from a high energy standard momentum AdS_2 scaling to a low energy regime where exponents found associated with momenta "backscattered" to a lower Brillioun zone in the extended zone scheme. We comment on how these findings can be used as a unique fingerprint for the detection of AdS_2 like "pseudogap metals" in the laboratory.

Contents

1 Introduction

The explanation of the difference between metals and insulators is one of the early successes of quantum mechanics. This is a very familiar affair: the periodic potential of the ions acts like a diffraction grating for the single electron wave functions, giving rise to gaps in the dispersion relations at the Brillioun zone boundary. Upon filling up the bands according to the Pauli principle, the Fermi energy can either end up in the middle of the bands or in the band gap, and the result is a Fermi-liquid metal or a band insulator, respectively. Recently, more than 75 years later, a metallic state of matter has been found

which appears to be completely unrelated to this free-fermion physics. Using a minimal bottom up AdS/CFT construction [1–3], it was discovered that a strongly interacting system of conformal fields when forced to finite (fermion) density turns into a metallic state that is controlled by an emergent, local quantum criticality [4]. The question arises how such a metal reacts to a static and periodic background potential. The low energy excitations are no longer behaving like quantum mechanical waves diffracting against the background potential. Instead, these are highly collective critical modes controlled by the emergent, purely temporal scale invariance.

In the AdS/CFT construction the strongly coupled conformal physics is described in terms of a gravitational dual consisting of Dirac fermions with special holographic boundary conditions, propagating in the Anti-de-Sitter Reissner-Nordström black hole (AdS-RN) background. Adding a spatially modulated potential turns out to be a highly complicated band structure-like problem, that we found intractable except in the limit of a weak potential. Exploiting perturbation theory using the strength of the potential as a small parameter we manage to solve the problem, and the outcomes are very surprising. The "domain wall" fermions of the AdS bulk dual to the propagating "background fermions" encoding for quasi-fermi surfaces in the boundary theory diffract in the usual way against the periodic potential giving rise to standard band gaps splitting the Fermi surfaces (Fig. 1, Fig. 5). However, the deep infrared associated with the AdS_2 near horizon geometry of the RN black hole which encodes for the fermion self-energy in the bulk is a completely different story. This is most clearly exposed in the "AdS_2 metal" regime. This the regime where the fermionic operators have such high scaling dimension that they never form Fermi surfaces in the deep IR despite the presence of a chemical potential. The low-frequency single fermion spectral function in the strongly coupled boundary CFT is in that case just proportional to the local quantum critical CFT_1 propagators associated with the near horizon AdS_2 geometry of the extremal AdS black hole coding for a non-zero chemical potential. They are therefore characterized by a scaling form $A(\omega, \vec{k}) \sim \omega^{2\nu_{\vec{k}}}$ with the particular holographic feature that the exponent is momentum dependent. The presence of a periodic potential causes these propagators to "hybridize" into a linear combination of CFT_1s. The consequence is that the effects of breaking translational symmetry are found in the *energy scaling* behavior of this "algebraic pseudo-gap" spectrum. At "high" energy where the weak potential does not exert influence one finds the usual $\omega^{2\nu_{\vec{k}}}$ scaling of the fermion spectral functions. The novel momentum dependence of the exponents persists and also the Umklapp momenta $\vec{K}$ end up in a similar exponentiated form. The effect is that upon descending in energy a cross-over follows to a regime governed by the smaller (less irrelevant) exponent $\nu_{\vec{k}-\vec{K}}$.

The question arises whether the "pseudogap metals" found in cuprate superconductors [5, 6] and the less well known manganites have anything to do with the AdS_2 metals [7–9].

To separate the technical details in the computation from the interesting physics that

the holographic single fermion spectral function in the presence of a lattice potential describes we will first summarize the physics of our results in the next section, which is hopefully also comprehensible for the non-experts. In Section 3-5 we will preform the detailed computation. Section 3 formulates the basic set-up for the holographic gravity system which encodes the lattice effect in terms of a modulated chemical potential and how a Dirac fermion probes this geometry to study the corresponding spectral function. In Section 4, we will recall how to obtain the $\omega \ll \mu_0$ retarded Green's function by the near-far matching method [4] and collect all the important ingredients. In section 5 we will compute the concrete semi-analytical full retarded fermion Green's function in the presence of a lattice. Some details are relegated to the appendix.

2 Summary of results and Outlook

The AdS/CFT dictionary strongly suggests that local quantum criticality is a robust feature of fermionic critical systems. The holographic encoding of critical finite density systems in terms of the gravitational bulk is natural and ubiquitous in that the finite chemical potential in the boundary simply dualizes to an electrical charge carried by a black hole in the AdS bulk. This AdS Reissner-Nordström black hole is extremal and it is distinctly characterized by an emergent near-horizon $\mathrm{AdS}_2 \times \mathbb{R}^d$ geometry (d is the number of space dimensions). This near-horizon region in turn governs the deep infrared of the field theory. What the "AdS_2" factor shows is that the deep infrared preserves criticality but only in purely temporal regards: through the duality it encodes a 0+1 dimensional CFT, a theory with dynamical critical exponent $z = \infty$ [4]. This "locally" quantum critical metallic behavior is quite suggestive with regard to the strange metals representing the central mystery in the condensed matter laboratories: both in the quantum critical heavy fermion systems and the normal state of optimally doped high $\mathrm{T_c}$ superconductors, experimental indications for such a behavior have been around for a long time.

The fermionic responses of this state can be studied by computing the single fermion propagators of the field theory, which dualize in infalling solutions of the Dirac equation in the bulk [1–3]. One of the main novelties of holographic dual description of finite density systems is that the (anomalous) scaling dimensions become arbitrary free parameters, rather than small deviations from near free field values. In the dual holographic description it is simply the mass parameter of the field in the AdS bulk. Pending the charge to mass ratio of the Dirac field, one then finds quite different behaviors. When the charge is much smaller than the Dirac mass in the bulk, corresponding to highly irrelevant scaling dimensions Δ of the fermion fields at zero density, one finds that the fermion spectral densities ($\mathrm{Im}G(\omega, k)$) at low ω/μ are directly proportional to the infrared CFT_1 densities

($\mathrm{Im}\mathcal{G}(\omega,k)$) associated with the AdS_2 near horizon geometry [4]:

$$\mathrm{Im}G(\omega,k) \simeq \mathrm{Im}\mathcal{G}(\omega,k) = \mathrm{Im}c_k e^{i\phi_k}\omega^{2\nu_k} \quad \text{with} \quad \nu_k = \sqrt{\frac{2k^2}{\mu^2} + \frac{m^2}{6} - \frac{q^2}{3}} \tag{2.1}$$

where the ultraviolet ($\mu = 0$) scaling dimension of the fermionic operator Δ is related to the mass in units of the AdS radius as $\Delta = mL + \frac{d}{2}$ and q is the fermion charge. The oddity of this "AdS_2 metal" is that the momentum dependence enters exclusively through the momentum dependence of the *infrared* scaling dimensions ν_k. In the small charge-to-mass regime ν_k is always positive, and one therefore finds at all momenta an "algebraic pseudo gap" at the chemical potential, where just the algebraic rise of density of states is momentum dependent. Although this pure "AdS_2 metal" gets less attention — presumably because it looks quite unfamilar — it is a serious part of the anti-de-Sitter/condensed matter (AdS/CMT) agenda. For instance, the AdS_2 metal appears to be generic outcome of fermions in top-down implementations of AdS/CFT where the weakly coupled system known in detail [10–12].

In the other scenario, when the charge-to-mass ratio is large one enters a different regime[1] characterized by "quasi Fermi-surfaces" defined by the appearance of poles in the retarded Green's function $G(\omega,k)$. For small ω/μ one can show that in this regime the holographically computed Green's function behaves as [2–4]

$$\begin{aligned} G(\omega,k) &\simeq \frac{Z}{v_F(k-k_F) - \omega - \Sigma(\omega,k)} + \ldots, \\ \Sigma(\omega,k) &= c_k e^{i\phi_k}\omega^{2\nu_k} + \ldots. \end{aligned} \tag{2.2}$$

Here the AdS_2 deep infrared enters as a non-(Landau-)Fermi-liquid self energy, while the Fermi-surface information is encoded as if there is a free Fermi gas decaying into this critical infrared [13]. In the bulk the origin of the emergent nearly free Fermi gas is clear. There the emergence is "geometrized" into the existence of Dirac fermions living at zero energy at the geometrical domain wall which interpolates between the 3+1 dimensional critical theory in the UV and the 0+1 dimensional local critical theory in the IR. The appearance of these quasi-Fermi surfaces simultaneously signals the proximity to "fermion hair" instabilities in the bulk (the electron star [14, 15], Dirac hair [16, 17] or quantum fermion models [18, 19]) dual to the instability of the AdS_2 metal in the boundary towards a stable fermionic state, which appears to be a real Fermi-liquid.

We now wish to ask the question: how do both these non-Fermi-liquid metals react to the presence of a static periodic potential characterized by a wave-vector of order of the Fermi-momentum? This is complementary to recent similar studies of lattice effects in holographic duals of strongly coupled theories: Hartnoll and Hofman consider the lattice

[1] There is also an intermediate oscillatory region where the spectral function is a periodic funciton of $\ln\omega$ and it has a non-vanishing weight at $\omega = 0$ [4]. We will not consider this regime here.

effect on momentum relaxation and show that it equals $\Gamma \sim T^{2\Delta_{k_L}}$ with Δ_{k_L} the scaling dimension of the charge density operator $J(\omega, k)$ in the locally critical theory at the lattice momentum k_L [20]. From the momentum relaxation one can directly extract the DC conductivity. The broadening of $\omega = 0$ delta-function into a Drude peak in the AC conductivity due to lattice effects was numerically studied by Horowitz, Santos and Tong with the remarkable observation that the holographic computation has a lot in common with experimental results in cuprates [21]. Similar to the latter study, we shall use a simple and natural encoding of a spatially varying static "lattice potential". One just adds a spatial variation of the electric field on the black hole horizon, dualizing into a spatial variation of the chemical potential in the boundary field theory. This approach was first introduced by Aperis *et al.* [22] and Flauger *et al.* [23]. who considered the responses of scalar fields in the regime where the periodicity of the potential is large compared to the intrinsic length scales of the system. Here we will focus in on the fermionic responses, where the wavevector of the periodic modulation is of order of the chemical potential, i.e. of order of the the Fermi momentum when a Fermi surface is formed. Spatially modulated chemical potentials are also considered in different holographic contexts in e.g. [24–29].[2] We will assume that this is a simple unidirectional potential with only a one-dimensional periodicity,

$$\mu(x, y) = \mu_0 + 2\epsilon \cos(\frac{x}{a}), \tag{2.3}$$

corresponding with an Umklapp wavevector (lattice momentum) in momentum space $K = 1/a$.

This corresponds to a bulk problem which is conceptually simple, but technically quite hazardous (section 3-5). Firstly, this spatial modulation of the electric charge would correspond to a non-spherically symmetric black-hole. We shall ignore this backreaction, which ought to be a good approximation as long as $\epsilon \ll \mu_0$.[3] In the present approximation, the free Dirac fermions in the bulk experience this electrical field modulation just as a diffracting potential in a spatial direction. On the other hand, the curved geometry along the radial direction and the boundary conditions associated with the dictionary translate this to a very complicated "band structure" problem in the bulk that we did not manage to tackle in general. However, as in the case of elementary band structure, it is expected that the weak potential scattering limit is representative for its most salient effects. Using ϵ/μ_0 again as the small parameter, we performed a weak potential scattering perturbation theory for the fermions in the bulk. As will be explained in section 4, this second approxi-

[2] Different ways to encode lattices in holographic set-ups are with intersecting branes [30] and holographic monopoles [31].

[3] The numerical results by Horowitz, Santos and Tong [21] do include the full backreaction but they needed a spatially varying scalar field to induce a modulation in the chemical potential. We have been informed that they also have numerical results for the full backreacted geometry in the set-up we use here. It would be interesting to compare our analytic predictions with their numerical work.

mation still corresponds with a surprisingly tedious problem that we nevertheless managed to solve qualitatively.

The outcomes are quite unexpected and to emphasize the physics over the technical steps we summarize them here. The predictable part is associated with the domain wall fermions responsible for the background free-fermion dispersion in Eq. (2.2). These react to the presence of the periodic potential just as free fermions. For a unidirectional potential along the x-direction we find that a bandgap opens in the "background" dispersion right at the scattering wavevector (K, k_y). For small ϵ the size of the gap behaves as (see (5.5)),

$$\Delta(K, k_y) \simeq \epsilon \sqrt{1 - \frac{1}{\sqrt{1 + (2\frac{k_y}{K})^2}}}. \tag{2.4}$$

The band gap is vanishing for this unidirectional potential when the transversal momentum $k_y = 0$. This might look unfamiliar but holographic fermions have a chiral property that causes them to react to potentials in the same way as the helical surface states of three dimensional topological insulators: at $k_y = 0$ the gap disappears since such fermions do not scatter in a backward direction. The new quasi-Fermi-surface in the presence of the weak potential can now be constructed as usual (Fig. 1). The Umklapp surfaces are straight lines in the k_y direction, centered at the Umklapp momenta. The gaps are centered at these Umklapp surfaces and when these intersect the Fermi-surface, the latter split in Fermi-surface "pockets", see Fig. 1.

The deep infrared AdS_2 sector is the interesting part. Although in a less direct way, one can discern that the physics in the bulk is still about the "hybridization" of free Dirac waves at momenta $\vec{k}$ and $\vec{k} \pm \vec{K}$, just as in the weak potential scattering problem of the solid state textbooks. The meaning of this hybridization in the dual field theory is however quite surprising. The AdS/CFT dictionary associates the free problem in the bulk with the physics of strongly interacting conformal fields in the boundary. In the deep infrared $AdS_2 \times \mathbb{R}^2$ in the absence of a lattice, one associates an *independent* CFT_1 to every point in momentum space (cf. Eq. (2.1)).[4] Upon breaking the continuous translational invariance, these CFT_1's start to interact and this has interesting consequences. As it corresponds in essence with quantum mechanical level mixing or hybridization in the bulk, we suggest to call the physics in the boundary "hybridization" as well, but the novelty is the way that this now refers to the reorganization of the locally critical CFT_1's.

The holographic solution of this problem of "weak potential" hybridization of CFT_1's is as follows (section 5). The CFT_1 propagator, either associated with the AdS_2 metal spectral density or the quasi Fermi-surface regime self energy, "hybridizes" due to the

[4]The CFT_1's are not completely independent. From the Green's function of the system, one reads of that they are spatially correlated over a length scale $\xi_{space} = \frac{\sqrt{2}}{\mu \nu_{k=0}}$ [32].

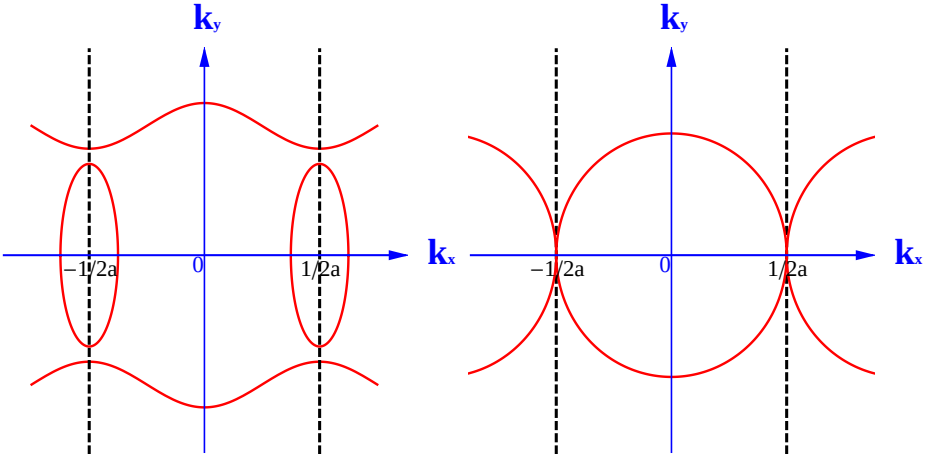

Figure 1. A cartoon of our results of the band structure for different k_F. The system under consideration has a lattice structure only in x direction. The red line curve is the Fermi surface ($\omega = 0$) and the black dashed line is the first BZ boundary. The left plot is for $k_F > \frac{K}{2}$ and the right plot is for $k_F = \frac{K}{2}$. We have a band gap at the first Brillouin Zone boundary $k_x = \pm\frac{K}{2}$ (the black dashed line) for generic $k_F > \frac{K}{2}$ (i.e. $k_y \neq 0$) which will close when $k_F = \frac{K}{2}$ (i.e. $k_y = 0$) . At generic k_x, the self-energy receives a second order correction related to the lattice effect, i.e. $\Sigma = \alpha_{\vec{k}}\,\omega^{2\nu_{\vec{k}}} + \beta^{(-)}_{\vec{k}}\omega^{2\nu_{\vec{k}-\vec{K}}} + \beta^{(0)}_{\vec{k}}\omega^{2\nu_{\vec{k}}}\ln\omega + \beta^{(+)}_{\vec{k}}\omega^{2\nu_{\vec{k}+\vec{K}}} + \ldots$. (See Eq. (2.8)). Note that this picture is a result in the periodic Brillouin zone scheme.

Umklapp potential into a "linear combination",

$$\begin{aligned}\mathcal{G}(\omega,\vec{k}) &= \alpha_{\vec{k}}\mathcal{G}_0(\omega,\vec{k}) + \mathcal{G}_1(\omega,\vec{k}) \\ &= \alpha_{\vec{k}}\,\omega^{2\nu_{\vec{k}}} + \beta^{(-)}_{\vec{k}}\omega^{2\nu_{\vec{k}-\vec{K}}} + \beta^{(0)}_{\vec{k}}\omega^{2\nu_{\vec{k}}}\ln\omega + \beta^{(+)}_{\vec{k}}\omega^{2\nu_{\vec{k}+\vec{K}}} + \ldots \end{aligned} \tag{2.5}$$

The leading term with coefficient $\alpha_{\vec{k}}$ is the zero'th order result as before, and the amplitudes $\alpha_{\vec{k}}, \beta^{(\pm,0)}_{\vec{k}}$ are depending on UV data with $\beta \ll \alpha$ in general for $\epsilon \ll \mu_0$. (The complete answers are given in section 5.2.)

The physical meaning of Eq. (2.5) is as follows. Starting in the AdS_2 metal at the "high" energies where the potential is not exerting influence yet, one finds the usual scaling of fermion spectral function in the "algebraic pseudogap" fashion $\sim \omega^{2\nu_{\vec{k}}}$. However, at some scale associated with the ratio of the prefactors $\beta^{(\ldots)}_{\vec{k}}$ a cross over follows to the "less irrelevant" $\sim \omega^{2\nu_{\vec{k}-\vec{K}}}$; since $\nu_{\vec{k}} \sim k$ the "hybridization of the CFT_1's" implies that the CFT_1's associated with the Brillioun zone with an index lower by one K in the extended zone scheme takes over at low energy. In this way, the periodic potential gets completely encoded in the energy scaling behavior of the electron propagators! Stepping back in the extended zone all the way to the first Brillioun zone one encounters an oddity: one cannot subtract a further K and therefore in the first zone the $\omega^{2\nu_{\vec{k}-\vec{K}}}$ contribution is not present. The ramification is that instead the next order in the scaling hierarchy takes over: in the first zone one finds instead a crossover to the $\omega^{2\nu_k} + \omega^{2\nu_k}|\ln(\omega)|$ scaling (Fig. 2). This

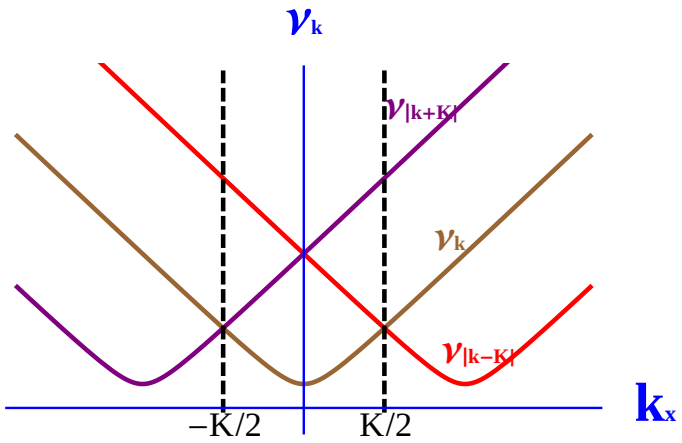

Figure 2. The behavior of the different powers of $\omega^{2\nu_{k-K}}, \omega^{2\nu_k}, \omega^{2\nu_{k+K}}$ in the lattice AdS_2-metal spectral function as a function of k. The IR of the Green's function is controlled by the lowest branch: $\omega^{2\nu_{k+K}}$ in the $\ell = -1$ Brillioun zone, $\omega^{2\nu_k}$ in the $\ell = 0$ Brillioun zone, and $\omega^{2\nu_{k-K}}$ in the $\ell = 1$ Brillioun zone.

logarithmic correction is easily understood as the leading term in the expansion

$$\omega^{2\nu_k(\mu)} = \omega^{2\nu_k(\mu_0)}(1 - 4k^2\delta\mu(x,y)\ln\omega + \ldots); \tag{2.6}$$

it is present in the higher Brillioun corrections as well, but for $\ell > 0$ these corrections are subleading compared to the Umklapp correction. The logarithmic correction has an interesting collusion right at the Brillioun zone boundary. Due to the "resonant" condition in the bulk, at the boundary yet another scaling arises, associated with a factor $\omega^{2\nu_k}|\ln(\omega)|^2$. This takes over in the deep IR at the first Brillioun zone boundary, in a regime $\delta k_x \ll \nu_k/|\ln(\omega)|$, where δk_x denotes the deviation of the momentum from the boundary of the first Brillioun zone. This understanding allows us to immediately guess what the answer will be at higher order in perturbation theory. At every next order in perturbation theory one can Umklapp to one further Brillioun zone:

$$\begin{aligned}\mathcal{G}_{\rm full}(\omega,\vec{k}) \sim \omega^{2\nu_{\vec{k}}} &+\epsilon^2(\omega^{2\nu_{\vec{k}-\vec{K}}} + \omega^{2\nu_{\vec{k}+\vec{K}}}) + \epsilon^4(\omega^{2\nu_{\vec{k}-2\vec{K}}} + 2\omega^{\nu_{\vec{k}+2\vec{K}}}) \\ &+\ldots+\epsilon^{2n}(\omega^{2\nu_{\vec{k}-n\vec{K}}} + \omega^{2\nu_{\vec{k}+n\vec{K}}}) + \ldots.\end{aligned} \tag{2.7}$$

This phenomenon of Umklapp imprinting on the scaling behavior of the fermion propagators is most easily discerned in the AdS_2 metal. As we already emphasized, the AdS_2-metal is the ultimate "algebraic pseudo-gap" state, where the fermion spectra are characterized by pseudogaps at all momenta, but where the algebraic rise of the spectral function is characterized by the momentum dependence of the exponents. This result therefore predicts that upon adding a periodic potential, the power law responses acquire generically subdominant corrections. However, in the deep IR it is these subdominant corrections

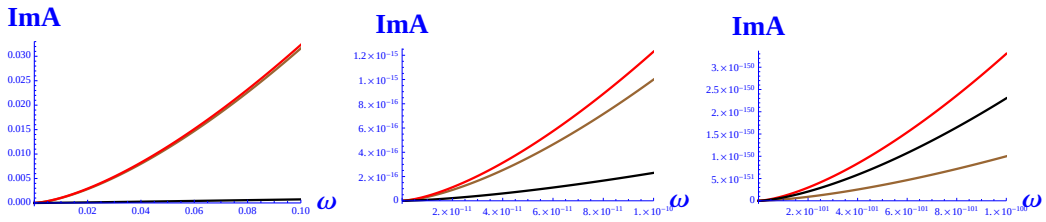

Figure 3. This sequence of AdS_2 metal spectral functions for a fixed generic k shows how the Umklapp contribution takes over at low frequencies. For $\ell = 0$, inside the 1st BZ, we show the full corrected spectral function $A_{\rm full}(\omega, \vec{k}) \sim {\rm Im}G$ (red), the original "bare" holographic spectral function $A_{\text{pure AdS}}(\omega, \vec{k}) \sim {\rm Im}G_0$ (brown), and the Umklapp correction due to the periodic chemical potential modulation $\delta A_{\rm lattice}(\omega, \vec{k}) \sim {\rm Im}\delta G$ (black).

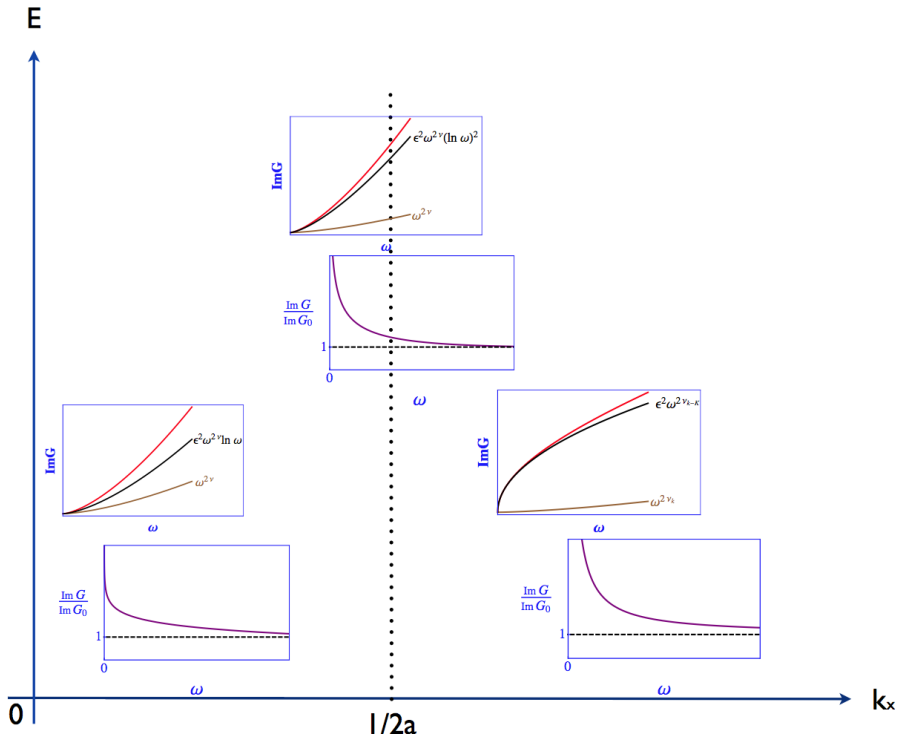

Figure 4. The behavior of the AdS_2 metal. The spectral function in three distinct regimes: the first Brillion zone, the Brillioun edge and higher Brillioun zones. In each case the full spectral function ${\rm Im}G(\omega, \vec{k}) = {\rm Im}G_0 + {\rm Im}\delta G$ is plotted in red, the "bare" component G_0 in brown and the Umklapp contribution, ${\rm Im}\delta G$ in black. The frequency scale is chosen such that the contributions are comparable by zooming as in Fig. 3. Below the ratio of the full spectral function in units of the "bare" spectral function is plotted for the full range of frequencies. This shows the excess states at low frequency that appear due to the lattice.

which control the density of states (Fig.4). Consistency argues that this can only be an enhancement of the number of states at low energy (otherwise there would be a zero in the spectral weight at small but finite ω). In the first Brillioun zone ($\ell = 0$) the logarithmic

correction which becomes dominant when $|\omega| \lesssim \epsilon |\ln |\omega||$ just accounts for the correction $\delta\mu(x, y)$. But in the higher Brillioun zones it is a true Umklapp correction which becomes dominant when $\omega \lesssim \epsilon$.

In the other regime, when $q \gg m$ and the system has quasi-Fermi surfaces to start, these effects are somewhat masked but they are still at work. Now the CFT_1 propagators modified by the potential determine the self-energy (2.2), i.e.

$$\begin{aligned}\Sigma(\omega, \vec{k}) &= \alpha_{\vec{k}} \Sigma_0(\omega, \vec{k}) + \Sigma_1(\omega, \vec{k}) \\ &= \alpha_{\vec{k}}\, \omega^{2\nu_{\vec{k}}} + \beta^{(-)}_{\vec{k}} \omega^{2\nu_{\vec{k}-\vec{K}}} + \beta^{(0)}_{\vec{k}} \omega^{2\nu_{\vec{k}}} \ln \omega + \beta^{(+)}_{\vec{k}} \omega^{2\nu_{\vec{k}+\vec{K}}} + \ldots . \end{aligned} \tag{2.8}$$

The lattice therefore alters the dispersive behavior of the "domain wall" free fermions. As we already argued, the latter react as usual to the potential by forming band gaps, but in addition one has the AdS_2 "heat bath" that reacts independently: it does not gap; the lattice only modifies its energy scaling. Since the modification entails extra states at low energies, the lattice enhances the dispersion of "domain wall" fermions and they become less well-defined.

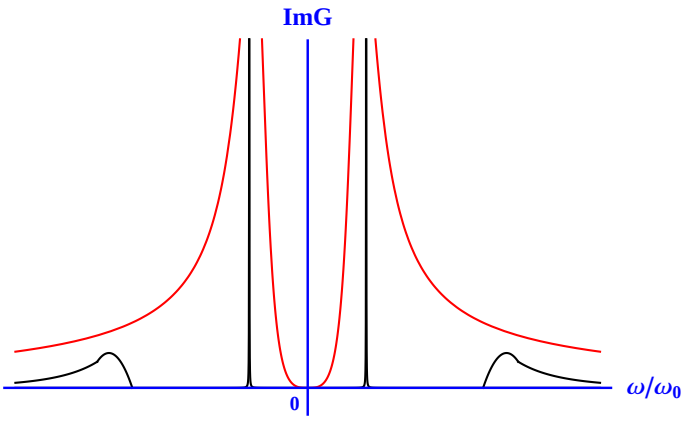

Figure 5. A cartoon of the dispersion driven pseudogap: standard band gap (black)vs a pseudogap driven by self-energy corrections that persist to the lowest frequencies (red), i.e. the spectral function is only singular at one point right at the chemical potential.

This implies that also in this regime the hard gaps of free fermions turn into soft pseudogaps with a small but non-zero spectral weight extending all the way to lowest energies (Fig. 5). Due to the proximity of the free fermion poles the information regarding the modification of the AdS_2 sector as it resides in the self-energy appears in a somewhat scrambled form in the full fermion spectral functions but in principle it can be retrieved by careful analysis of the latter. An interesting general consequence of these results is that different from a real Fermi-liquid this quasi Fermi-surface "strange metal" *is not localizable by a periodic potential in a band insulator*. The AdS_2 deep infrared is just not describing diffraction of quantum mechanical waves, but instead it is about highly collective critical

functions that loose their purely temporal scale invariance when translational symmetry is broken, acquiring the energy scaling highlighted in Eq. (2.5) and Fig. 4. This is yet another way of sharply distinguishing the "quasi Fermi surface" strange metals from true Fermi-liquids. At present that the "hard wall" confining electron star as constructed by Sachdev [18] is the only obvious holographic encoding of a straightforward Fermi-liquid, and one infers immediately that in the boundary field theory the quasiparticles will react like the domain wall fermions, forming conventional hard gapped band insulators in principle. The physical argument put forward here would argue that in the true groundstate of the quasi-Fermi surface regime – the Lifshitz-type infrareds associated with the "deconfining" electron stars [15] – a similar soft pseudo-gap enhancement will happen in the presence of a periodic potential. These Lifshitz-type infrareds presumably encode for fractionalized Fermi surfaces which arise from Fermions interacting with a gaplless "heat-bath". Qualitatively this is similar to the AdS_2 bath in the AdS RN-BH set-up explored here. It remains an interesting open question to verify this.

Outlook

Perhaps the most interesting ramification of our findings is that they can be used as a *diagnostic* for the realization of holographic metals in laboratory systems. The main challenge of the AdS/CMT development is to find out whether the holographic strange metals have any relevancy towards the strongly interacting electron systems as realized in the condensed matter laboratories. It appears that the workings of periodic potentials, nesting and so forth, might be used as a potentially powerful diagnostic in this regard. Although we have only control over the weak potential limit, it appears that the most salient feature we have identified might be quite general: static potentials are encoded in the energy scaling, while the periodic potential information is encoded in the way that this scaling varies in the extended zone scheme. At the least it suggests a quite unconventional to analyze angular resolved photoemission data (ARPES); in a future publication we will address how these matters act out in the real space fermionic response as measured by scanning tunneling spectroscopy (STS).

ARPES gives in its standard mode access to the extended Brillioun zone. It is usually taken for granted that the electron spectral functions are (modulo the spectral weight) just copies of each other in different zones. This is actually a flawed intuition based on non-interacting fermions. For free fermions it is of course a fact that the periodicity of the potential in real space dualizes in a perfect periodicity in momentum space in the form of the extended Brillioun zone. Actually, this is also still the case for the Fermi-liquid in the scaling limit. Because of the adiabatic continuity, the emergent quasiparticles have to behave in this regard like the free fermions: although one sees many copies of the Fermi surface in the extended zone scheme, all Fermi-surfaces including their IR fixed point physics (e.g. the ω^2 self energies) are identical in all the zones. There is "only

one Fermi surface" in the Fermi liquid which can be measured in any zone, and the only variations that are allowed in the extended zone are associated with the spectral weights in the photoemission (the "shadow band" motive). However, in a true non-Fermi liquid where the adiabatic continuation is not at work, single particle momentum is no longer a meaningful quantum number and there is no fundamental reason for the system to be precisely periodic in the extended single particle momentum Brillioun zone. This is what one sees so clearly at work in the above holographic non Fermi-liquids! Quite generally, the non periodicity of the fermion spectral functions in the extended zone is therefore a direct experimental probe of the non-Fermi liquid nature of electron matter.

To find out whether the phenomenological marginal Fermi liquid behavior found in optimally doped cuprates has any relation with the AdS_2 metals [33], it would be quite interesting to study whether the self energies are actually varying going to higher Brillioun zones – to the best of our knowledge this has never been attempted systematically. Another empirical issue coming into view is whether the pseudogap features seen by e.g. ARPES and STS in underdoped cuprates have any dealing with an AdS_2 deep infrared while experiencing translational symmetry breaking potentials. A case has been evolving on the course of time that these pseudogaps behave in quite mysterious ways. A famous example is the "nodal-antinodal dichotomy", referring to the rather sharp change from relatively coherent, marginal Fermi-liquid behavior in a region in momentum space close to the "nodal points" where the massless Bogoliubov excitations are found in the superconductor, to a highly incoherent antinodal momentum space regime [6]. This sudden change seems to happen at the location of the Umklapp surface associated e.g. with the two sublattice antiferromagnetism of the insulating cuprates [6]. Could this be some strong potential version of the weak potential effects we have identified in this paper? Similarly, underdoped cuprates do have a reputation for "refusing to localize", as examplified by very slowly (logarithmically) diverging resistivities in the underdoped regime [34], the hardship to destroy superconductivity by well developed stripe order [35], etc. Much more work is needed to settle these issues.

Finally, our findings might also be instrumental to interrogate other systems that appear to be characterized by pseudogap single electron behavior. A problem for the experimentalists is that pseudogap-like behavior can easily arise as an experimental artefact, associated with bad surfaces and so forth. A point in case are the bilayer manganites. Famous for their colossal magneto-resistance effects, these are very bad metals at low temperature that have been around for a while as non-superconducting bad metals [36]. It first appeared that in the best samples one does find signs of very heavy but coherent Fermi-liquid quasiparticles [7], but recently it was demonstrated that these quasiparticles are actually artefacts of stacking faults [9]. The best manganite surfaces in fact show a quite neat pseudogap behavior throughout the Brillioun zone. Could these be realizations of the AdS_2 metal? We look forward to a very careful study of the scaling behavior of the

pseudogap: the AdS_2 metal should signal itself through an algebraic scaling behavior as function of energy which should show non-trivial variations in momentum space.

3 Lattice holographic metals through chemical potential modulation

We consider the most elementary holographic dual to a fermion system at a finite density in 2+1 dimensions. This is an extremal Reissner-Nordström black hole solution of the AdS Einstein-Maxwell-Dirac theory:

$$ds^2 = -r^2 f(r) dt^2 + \frac{dr^2}{r^2 f(r)} + r^2(dx^2 + dy^2), \tag{3.1}$$

$$A_t = \mu_0 \big(1 - \frac{1}{r}\big), \tag{3.2}$$

$$f(r) = 1 - \frac{1+Q^2}{r^3} + \frac{Q^2}{r^4}, \tag{3.3}$$

$$\mu_0 = 2Q, \tag{3.4}$$

where μ_0 denotes the chemical potential of the system. We have set both the cosmological radius and the horizon to unity. The Hawking temperature of this background is

$$T = \frac{1}{4\pi}(3 - Q^2). \tag{3.5}$$

We now wish to take lattice effects into consideration. We do so by simply modifying the chemical potential *alone*:

$$ds^2 = -r^2 f(r) dt^2 + \frac{dr^2}{r^2 f(r)} + r^2(dx^2 + dy^2), \tag{3.6}$$

$$A_t = \big[\mu_0 + \mu_1(x)\big] \big(1 - \frac{1}{r}\big), \tag{3.7}$$

$$f(r) = 1 - \frac{1+Q^2}{r^3} + \frac{Q^2}{r^4}, \tag{3.8}$$

$$\mu_0 = 2Q. \tag{3.9}$$

Here $\mu_1(x)$ is a small periodic potential which denotes the effect of the lattice. In the limit $\mu_1(x) \ll \mu_0$, we can ignore the backreaction of this weak nonuniform potential $\mu_1(x)$ to the background metric. Strictly speaking this is not a solution to the equations of motion of the system, even in a scaling limit. Nevertheless, if the energy density due to μ_1 is small, combined with the intuition that the lattice modulation should decrease into the interior and the knowledge that it is precisely the (qualitative) IR physics in the interior that we are interested in, ignoring the backreaction should be a reasonable approximation to the true physics [5]. In the following, we will study the system at zero temperature, i.e.

[5] This is similar to the case of [20] where the authors also assumed that the lattice effect is irrelevant and the IR physics is still governed by the AdS_2 geometry. In a qualitatively similar setup where the lattice periodicity is imposed through a periodic modulation of a scalar order parameter which backreacts

$Q = \sqrt{3}$ and the result we obtain should be a good approximation to the finite but low temperature case. For simplicity, we shall only consider a one-dimensional lattice with the other direction continuous.

Such a periodic potential $\mu_1(x) = \mu_1(x + 2\pi a)$ ought to capture the leading effect of the weak potential generated by periodically spaced sources (ion cores). For the sake of simplicity and to grasp the main feature of the system we can approximate $\mu_1(x)$ by a simple $\cos(\frac{x}{a})$ function. This lowest frequency contribution in the Fourier series of $\mu_1(x)$ is usually also the largest contribution. This kind of approximation also corresponds to the nearest neighbor approximation in momentum space. In fact, we know that in the weak potential limit of a condensed matter lattice system, the boundary of the n-th Brilliouin zone will open a gap whenever the n-th Fourier coefficient in the Fourier series of the potential is not zero. To analyze the effect of the periodic potential to the holographic system, the lowest order term in the Fourier series of $\mu_1(x)$ can already capture the interesting physics that we want to show. Thus we choose [6]

$$\mu_1(x) = 2\epsilon \cos \frac{x}{a}. \tag{3.10}$$

with $\epsilon \ll \mu_0$ the small parameter that controls the modulation.

We probe this zero-temperature periodically modulated background with a Dirac fermion with mass m and charge q:

$$(\Gamma^a e_a{}^\mu \mathcal{D}_\mu - m)\Psi = 0 \tag{3.11}$$

where $\mathcal{D}_\mu = \partial_\mu + \frac{1}{4}\omega_{ab\mu}\Gamma^{ab} - iqA_\mu$ and the indices μ and a denote the bulk spacetime and tangent space index respectively. The Dirac field corresponds to a fermionic operator of dimension $\Delta = \frac{3}{2} + m$ in the field theory. Solving the Dirac equation with infalling boundary condition at the horizon for Dirac field, we can extract the field theory two-point retarded Green's function for this fermionic operator by the AdS/CFT dictionary.

To solve the Dirac equation we choose a basis of gamma matrices

$$\Gamma^{\underline{t}} = \begin{pmatrix} i\sigma^1 & 0 \\ 0 & i\sigma^1 \end{pmatrix}, \quad \Gamma^{\underline{r}} = \begin{pmatrix} -\sigma^3 & 0 \\ 0 & -\sigma^3 \end{pmatrix}, \quad \Gamma^{\underline{x}} = \begin{pmatrix} -\sigma^2 & 0 \\ 0 & \sigma^2 \end{pmatrix}, \quad \Gamma^{\underline{y}} = \begin{pmatrix} 0 & -i\sigma^2 \\ i\sigma^2 & 0 \end{pmatrix}. \tag{3.12}$$

on both the gauge field and the geometry [21] the numerical solution shows explicitly that in the deep IR is indeed governed by the AdS_2 geometry. The authors of [21], who have also numerically solved the chemical potential modulation set-up we employ here, have privately communicated to us that this indeed also happens here as surmised.

Alternatively, In our case, one could imagine adding a neutral sector whose energy density is periodic with precisely the opposite phase. Even in cases where the backreaction of a periodic potential may change the geometry qualitatively, the feature of hybridyzation will not change as this is only related to the fact that we are considering the nearest neighbor interaction in the momentum space. What will change, if the backreaction changes qualitatively is all results that depend on the near-horizon AdS_2 geometry.

[6] Note that the gauge field's equation of motion is also satisfied as long as $\mu_1(x)$ is a harmonic function and here we are choosing the largest Fourier contribution in $\mu_1(x)$ to the harmonic function as a proper approximation.

A redefinition of Ψ

$$\Psi(t,r,x,y) = (-gg^{rr})^{-\frac{1}{4}} \begin{pmatrix} \Phi_1 \\ \Phi_2 \end{pmatrix}, \tag{3.13}$$

with each $\Phi_\alpha,\ \alpha = 1,2$ a two-component spinor effectively removes the spin connection from the equation of motion [2]. Due the explicit x-dependence in $\mu_1(x)$ the different momentum modes are no longer independent, but will mix those which differ by an inverse lattice vector $K = 1/a$. At the same time, the periodicity in the x-direction due to $\mu_1(x)$ ought to reflect itself in the solutions Φ_α. These features can be accounted for by a Bloch expansion

$$\Phi_\alpha = \int \frac{d\omega dk_x dk_y}{2\pi} \sum_{\ell \in \mathrm{Z}} \Phi_\alpha^{(\ell)}(r,\omega,k_x,k_y) e^{-i\omega t + i\left[(k_x+\ell K)x + k_y y\right]}, \quad \alpha = 1,2, \tag{3.14}$$

where $k_x \in [-\frac{K}{2}, \frac{K}{2}]$ and ℓ characterizes the momentum level or Brillouin zone.

In Bloch waves, the Dirac equation of motion reduces to

$$\begin{aligned} &(\partial_r + m\sqrt{g_{rr}}\sigma^3)\Phi_\alpha^{(\ell)} - i\sqrt{\frac{g_{rr}}{g_{tt}}}\left(\omega + q\mu_0(1-\frac{1}{r})\right)\sigma^2\Phi_\alpha^{(\ell)} - (-1)^\alpha\sqrt{\frac{g_{rr}}{g_{xx}}}(\frac{\ell}{a}+k_x)\sigma^1\Phi_\alpha^{(\ell)} \\ &-i(-1)^\alpha\sqrt{\frac{g_{rr}}{g_{xx}}}k_y\sigma^1\Phi_\beta^{(\ell)} - iq\epsilon\sqrt{\frac{g_{rr}}{g_{tt}}}\sigma^2(1-\frac{1}{r})(\Phi_\alpha^{(\ell-1)} + \Phi_\alpha^{(\ell+1)}) = 0, \end{aligned} \tag{3.15}$$

where $\alpha = 1,2; \beta = 3-\alpha$ and ϵ is the Fourier coefficient in $\mu_1(x) = 2\epsilon\cos\frac{x}{a}$. We explicitly see how the periodicity mixes modes whose momentum differ by K. As a result, the momentum is no longer conserved and, as is well known, only k_x is the conserved quantity.

4 Retarded Green's function

We now solve the EOM (3.15) with the infalling boundary condition for each $\Phi_\alpha^{(\ell)}$ to extract the corresponding retarded Green's function in the dual strongly interacting boundary field theory. From (3.15), we can see that generally the different spinor components of the Dirac field mix with each other for nonzero k_y. To simplify the equations, we make the following rotation in $\alpha,\ \beta$ space (recall that each Φ_α is still a two-component spinor and it is in that spinor space that the Pauli matrices act. This transformation rotates the two separate two-component spinors into each other.)

$$\begin{pmatrix} \frac{(k_x+\frac{\ell}{a}+k_\ell)}{\sqrt{k_y^2+(k_x+\frac{\ell}{a}+k_\ell)^2}} & \frac{ik_y}{\sqrt{k_y^2+(k_x+\frac{\ell}{a}+k_\ell)^2}} \\ \frac{i(-k_x-\frac{\ell}{a}+k_\ell)}{k_y\sqrt{1+(k_x+\frac{\ell}{a}-k_\ell)^2/k_y^2}} & \frac{1}{\sqrt{1+(k_x+\frac{\ell}{a}-k_\ell)^2/k_y^2}} \end{pmatrix} \begin{pmatrix} \Phi_1^{(\ell)} \\ \Phi_2^{(\ell)} \end{pmatrix} \to \begin{pmatrix} \Phi_1^{(\ell)} \\ \Phi_2^{(\ell)} \end{pmatrix}, \tag{4.1}$$

where $k_\ell = \sqrt{(k_x+\frac{\ell}{a})^2 + k_y^2}$. When $k_y \to 0$, this transformation matrix is $\begin{pmatrix} 1 & 0 \\ 0 & 1 \end{pmatrix}$ for $k_x > 0$, while $\begin{pmatrix} 0 & i \\ i & 0 \end{pmatrix}$ for $k_x < 0$.

After this rotation, the equation of motion (3.15) simplifies to

$$(\partial_r + m\sqrt{g_{rr}}\sigma^3)\Phi_\alpha^{(\ell)} - i\sqrt{\frac{g_{rr}}{g_{tt}}}(\omega + q\mu_0(1-\frac{1}{r}))\sigma^2\Phi_\alpha^{(\ell)} - (-1)^\alpha\sqrt{\frac{g_{rr}}{g_{xx}}}k_\ell\sigma^1\Phi_\alpha^{(\ell)}$$
$$-iq\epsilon\sqrt{\frac{g_{rr}}{g_{tt}}}\sigma^2(1-\frac{1}{r})\sum_{\beta;\ell'=\ell\pm1} M_{\alpha\beta,\ell\ell'}\Phi_\beta^{(\ell')} = 0, \tag{4.2}$$

with $M_{\alpha\beta,\ell\ell'} = (M_{\alpha1,\ell\ell'}, M_{\alpha2,\ell\ell'})$ and

$$M_{\alpha1,\ell\ell'} = -i^{3-\alpha}\text{sign}(k_y^{3-\alpha})\frac{\left(\frac{\ell-\ell'}{a} + k_\ell - (-1)^\alpha k_{\ell'}\right)\sqrt{k_{\ell'}^2 - (-1)^\alpha k_{\ell'}(k_x + \frac{\ell'}{a})}}{2k_{\ell'}\sqrt{k_\ell^2 + k_\ell(k_x + \frac{\ell}{a})}},$$
$$M_{\alpha2,\ell\ell'} = (-i)^\alpha\text{sign}(k_y^\alpha)\frac{\left(\frac{\ell-\ell'}{a} - k_\ell - (-1)^\alpha k_{\ell'}\right)\sqrt{k_{\ell'}^2 - (-1)^\alpha k_{\ell'}(k_x + \frac{\ell'}{a})}}{2k_{\ell'}\sqrt{k_\ell^2 - k_\ell(k_x + \frac{\ell}{a})}}. \tag{4.3}$$

Note that $M_{\alpha\beta,\ell\ell'}$ have smooth limits as $k_y \to 0$. This rotation makes explicit that mixing of the different levels is controlled by k_ℓ. In terms of symmetries, the coupling between different momentum levels is related to the continuous translational symmetry breaking in the x direction while the mixing between different spinor indices is related to the broken $SO(2)$ symmetry in the x, y plane.

Equation (4.2) describes a set of infinite coupled equations with infinite many fields to be solved, corresponding to the full range of $\ell = 0, \pm1, \pm2, ..., \pm\infty$. In principle we need to diagonalize these equations to solve them. To do so explicitly is non-trivial because of the r-radial coordinate dependence of the coefficients in the equation. Instead we shall solve them in perturbation theory in the limit $\epsilon \ll \mu_0$. For ϵ is a small parameter, we can solve the EOM (4.2) order by order in ϵ in the whole spacetime.

Expanding each level $\Phi_\alpha^{(\ell)}$ in ϵ as

$$\Phi_\alpha^{(\ell)} = \Phi_\alpha^{(0,\ell)} + \epsilon\Phi_\alpha^{(1,\ell)} + \epsilon^2\Phi_\alpha^{(2,\ell)} + ... \tag{4.4}$$

the zeroth order equation is just the free Dirac equation without the interaction term, and each level ℓ decouples at this order.

$$(\partial_r + m\sqrt{g_{rr}}\sigma^3)\Phi_\alpha^{(0,\ell)} - i\sqrt{\frac{g_{rr}}{g_{tt}}}(\omega + q\mu_0(1-\frac{1}{r}))\sigma^2\Phi_\alpha^{(0,\ell)} - (-1)^\alpha\sqrt{\frac{g_{rr}}{g_{xx}}}k_\ell\sigma^1\Phi_\alpha^{(0,\ell)} = 0, \tag{4.5}$$

Substituting the lowest order solutions into the first order equation to obtain the first order equations, we obtain the hierarchy of equations

$$(\partial_r + m\sqrt{g_{rr}}\sigma^3)\Phi_\alpha^{(s,\ell)} - i\sqrt{\frac{g_{rr}}{g_{tt}}}(\omega + q\mu_0(1-\frac{1}{r}))\sigma^2\Phi_\alpha^{(s,\ell)} - (-1)^\alpha\sqrt{\frac{g_{rr}}{g_{xx}}}k_\ell\sigma^1\Phi_\alpha^{(s,\ell)}$$
$$- iq\sqrt{\frac{g_{rr}}{g_{tt}}}\sigma^2(1-\frac{1}{r})\sum_{\beta;\ell'=\ell\pm1} M_{\alpha\beta,\ell\ell'}\Phi_\beta^{(s-1,\ell')} = 0 \tag{4.6}$$

with $s = 1, 2, \ldots$

Previous studies have shown that the relative size of q to m determines the characteristics of the system [3, 4]. We shall assume that this will remain the case with the lattice modulation and use this liberty to choose $m = 0$ from here on.

4.1 Boundary conditions

To compute the retarded field theory Green's function we need to impose infalling boundary conditions at the extremal horizon $r \equiv r_h = 1$.[7] The number of linearly independent infalling boundary conditions are equal to the number of fields in the system, which is formally infinite. Because the fields in the system can be labeled by the level ℓ and the spinor component α, we can also label the boundary conditions using $\alpha\ell$. The following is the definition of the $\alpha\ell$-th boundary condition: we pick a single infalling spinor component at zeroth order: $\Phi_\alpha^{(0,\ell)}(r_h) \neq 0$ for a fixed component α and fixed level ℓ with the other component and all other levels vanishing. At lowest order in ϵ, all other modes decouple from these boundary conditions and only the field $\Phi_{\alpha^{\text{fix}}}^{(0,\ell^{\text{fix}})}(r)$ will be non-zero. At the first order in ϵ, we can see from the equations (3.15) and (4.2) that now also the fields $\Phi_{\alpha^{\text{fix}}}^{(1,\ell^{\text{fix}}\pm1)}(r)$ are nonzero when $k_y = 0$ and when $k_y \neq 0$ both $\Phi_{\alpha^{\text{fix}}}^{(1,\ell^{\text{fix}}\pm1)}(r_h)$ and $\Phi_{\beta^{\text{fix}}\neq\alpha^{\text{fix}}}^{(1,\ell\pm1)}(r_h)$ are nonzero. At the second order, we also excite $\Phi_\alpha^{(2,\ell^{\text{fix}}\pm1\pm1)}(r_h)$ and $\Phi_\beta^{(2,\ell^{\text{fix}}\pm1\pm1)}(r_h)$. When we excite these higher order modes, we should also impose infalling boundary conditions for these modes. As we shall see, it will suffice for us to compute the solution up to second order only.

Letting ℓ^{fix} and α^{fix} range over all possible values, we obtain an infinite set of linearly independent boundary conditions. Thus one can get the most general solution to the Dirac equation with infalling boundary conditions. The full solution is therefore an $\infty \times \infty$ matrix $\Phi^{(s)}_{\alpha\ell(\beta\ell')}(r)$, whose $\alpha\ell\beta\ell'$ element gives the solution $\Phi_\alpha^{(s,\ell)}(r)$ under the $\beta\ell'$-th infalling horizon boundary condition.

At AdS infinity — the conformal boundary at $r \to \infty$ corresponding to the UV in the field theory — the equations of all levels and all orders $\Phi_\alpha^{(s,\ell)}$ decouple and are of the same form as the free Dirac equation, i.e. for any $\beta\ell'$-th horizon boundary condition all $\Phi_\alpha^{(s,\ell)}$ behave on the conformal boundary as

$$\Phi^{(s)}_{\alpha\ell(\beta\ell')} = A^{(s)}_{\alpha\ell,\beta\ell'} r^m \begin{pmatrix} 0 \\ 1 \end{pmatrix} + B^{(s)}_{\alpha\ell,\beta\ell'} r^{-m} \begin{pmatrix} 1 \\ 0 \end{pmatrix} + \ldots \tag{4.7}$$

Note that the superscript (s) means the order of ϵ, and not the Bloch wave indexed by ℓ. The retarded Green's function is then computed from these two matrices $A_{\alpha\ell,\beta\ell'} \equiv \sum_s \epsilon^s A^{(s)}_{\alpha\ell,\beta\ell'}$ and $B_{\alpha\ell,\beta\ell'} \equiv \sum_s \epsilon^s B^{(s)}_{\alpha\ell,\beta\ell'}$ as

$$G_R = BA^{-1}. \tag{4.8}$$

[7] We have chosen $\mu_0 = 2\sqrt{3}$.

The spectral weight can be easily obtained from the Green's function matrix. In the following we focus on the diagonal momentum Green's function $G_R(\omega; \vec{k}, \vec{k})$ and therefore the diagonal momentum spectral weight [8]. In both A and B matrices, the leading order contribution to the off-diagonal elements are of order ϵ whereas the leading order contributions in the diagonal elements are of order ϵ^0. For consistency in determining the effect of $\mu_1(x)$ in the spectral weight up to the second order, we therefore have to keep both the zeroth and second order solutions in the diagonal elements of the solution matrix as well as the first order solution in the off diagonal elements. This way we see that the modulation $\mu_1(x)$ affects the diagonal momentum Green's function at the second order of ϵ. This is the case for a generic momentum k_x. At the boundary of the first Brillouin zone, we will need more care as we will see later.

Thus generally the A and B matrices look like

$$A_{\alpha\ell,\alpha'\ell'} = \begin{pmatrix} \ddots & & & & \\ & \epsilon F^A_{\alpha\alpha'} & & & \\ & (Z^A + \epsilon^2 S^A)\delta_{\alpha\alpha'} & \epsilon F^A_{\alpha\alpha'} & & \\ & \epsilon F^A_{\alpha\alpha'} & (Z^A + \epsilon^2 S^A)\delta_{\alpha\alpha'} & \epsilon F^A_{\alpha\alpha'} & \\ & & \epsilon F^A_{\alpha\alpha'} & (Z^A + \epsilon^2 S^A)\delta_{\alpha\alpha'} & \\ & & & \epsilon F^A_{\alpha\alpha'} & \\ & & & & \ddots \end{pmatrix},$$

$$B_{\alpha\ell,\alpha'\ell'} = \begin{pmatrix} \ddots & & & & \\ & \epsilon F^B_{\alpha\alpha'} & & & \\ & (Z^B + \epsilon^2 S^B)\delta_{\alpha\alpha'} & \epsilon F^B_{\alpha\alpha'} & & \\ & \epsilon F^B_{\alpha\alpha'} & (Z^B + \epsilon^2 S^B)\delta_{\alpha\alpha'} & \epsilon F^B_{\alpha\alpha'} & \\ & & \epsilon F^B_{\alpha\alpha'} & (Z^B + \epsilon^2 S^B)\delta_{\alpha\alpha'} & \\ & & & \epsilon F^B_{\alpha\alpha'} & \\ & & & & \ddots \end{pmatrix}, \quad (4.9)$$

where the zeroth, first and second order A and B coefficients $Z^{A,B}$, $F^{A,B}$ and $S^{A,B}$ do depend on ℓ and ℓ' in contrast to this sketch of their form.

In the following sections we will compute these two matrices using the near-far matching method.

[8] Since the lattice breaks translation invariance, momentum is no longer a good quantum number. The Green's function will therefore also have non-zero value for operators are momenta that differ by a lattice vector. Formally we should diagonalize the system into a new "non-momentum" basis of modes. Since one in ARPES experiments the photoelectron propagates in the galilean continuum it has a definite momentum, one keeps the Green's function in the momentum-basis. The dominant response is still in the diagonal momentum-channel, though this now contains a mixing with other momentum-modes.

4.2 Matching

The macroscopic properties of this system are determined by the low energy modes. We shall therefore focus on the small ω/μ_0 region. This enables us to use the near-far matching method to determine the spectral function following [4]. We divide the spacetime into two regions: the near region and the far region. The near region is the near horizon region, i.e. $r-1 \ll 1$. Here the geometry becomes that of $AdS_2 \times \mathbb{R}^2$.[9] The far region is defined as the $\frac{\omega/\mu_0}{r-1} \ll 1$ region. We can solve the equations in the near and far region separately. For $\omega \ll \mu_0$ the near and far region have a non-zero overlap $\omega/\mu_0 \ll r-1 \ll 1$ and we can match the separate approximations within this region.

We will first study the near horizon region in detail.

4.2.1 Near region solutions for $\Phi_\alpha^{(0,\ell)}$

The zeroth order solution (no lattice modulation) is the simplest case and the results were already obtained in [4, 37]. We collect their solutions here.

Near the horizon, we have $g_{tt} = g^{rr} \simeq 6(r-1)^2$ and $g_{xx} \simeq 1$. and the equation (4.2) for $\Phi_\alpha^{(0,\ell)}$ is by construction identical to extremal RN AdS black hole case with $k_\ell = \sqrt{(k_x + \frac{\ell}{a})^2 + k_y^2}$ [4]:

$$\partial_r \Phi_\alpha^{(0,\ell)} - \frac{i}{6(r-1)^2}(\omega + q\mu_0(r-1))\sigma^2 \Phi_\alpha^{(0,\ell)} - (-1)^\alpha \frac{1}{\sqrt{6}(r-1)} k_\ell \sigma^1 \Phi_\alpha^{(0,\ell)} = 0. \tag{4.10}$$

After performing a coordinate transformation, $x = \frac{\omega}{r-1}$, this first order spinor equation is equivalent to a second order one for each of the separate components:

$$\partial_x^2 \Phi_{\alpha j}^{(0,\ell)} + (\frac{2}{x} - \frac{\partial_x h_{\alpha j}}{h_{\alpha j}})\partial_x \Phi_{\alpha j}^{(0,\ell)} + \frac{h_{\alpha 1} h_{\alpha 2}}{x^4} \Phi_{\alpha j}^{(0,\ell)} = 0 \ . \tag{4.11}$$

Here

$$h_{\alpha j} = -x(\frac{x}{6} + \frac{q\mu_0}{6} + (-1)^{\alpha+j+1}\frac{k_\ell}{\sqrt{6}}) \tag{4.12}$$

and the equation is solvable [37] in terms of Whittaker functions.

For the two independent components of the spinor, we have the infalling solutions

$$\begin{aligned} \Phi_\alpha^{(0,\ell)} &= \begin{pmatrix} \Phi_{\alpha 1}^{(0,\ell)} \\ \Phi_{\alpha 2}^{(0,\ell)} \end{pmatrix} \\ &= \begin{pmatrix} c_{(\alpha,\text{in})} x^{-1/2} \left[-W_{\frac{1}{2}+i\frac{q\mu_0}{6},\nu_{k_\ell}}(-2i\frac{x}{6}) + \frac{i(-1)^\alpha k_\ell}{\sqrt{6}} W_{-\frac{1}{2}+i\frac{q\mu_0}{6},\nu_{k_\ell}}(-2i\frac{x}{6}) \right] \\ c_{(\alpha,\text{in})} i x^{-1/2} \left[W_{\frac{1}{2}+i\frac{q\mu_0}{6},\nu_{k_\ell}}(-2i\frac{x}{6}) + \frac{i(-1)^\alpha k_\ell}{\sqrt{6}} W_{-\frac{1}{2}+i\frac{q\mu_0}{6},\nu_{k_\ell}}(-2i\frac{x}{6}) \right] \end{pmatrix} \end{aligned} \tag{4.13}$$

[9] Recall that we are ignoring gravitational backreaction. However, because the breaking of translational invariance due to the lattice should be a UV effect, even with gravitational backreaction the strict near horizon IR region should be approximately $AdS_2 \times \mathbb{R}^2$. Physically we are interested in the qualitative effects due to the periodic potential and intuitively these should already be there with the periodically modulated electrostatic potential. Including the induced modulation in the spacetime curvature due to the varying energy-density in the electric field will presumably yield only quantitative and not qualitative changes.

and outgoing solutions:

$$\begin{pmatrix}\Phi^{(0,\ell)}_{\alpha 1}\\ \Phi^{(0,\ell)}_{\alpha 2}\end{pmatrix} = \begin{pmatrix} c_{(\alpha,\text{out})}x^{-1/2}\Big[- W_{\frac{1}{2}-i\frac{q\mu_0}{6},\nu_{k_\ell}}(2i\frac{x}{6}) - \frac{i(-1)^\alpha k_\ell}{\sqrt{6}} W_{-\frac{1}{2}-i\frac{q\mu_0}{6},\nu_{k_\ell}}(2i\frac{x}{6})\Big] \\ c_{(\alpha,\text{out})}ix^{-1/2}\Big[- W_{\frac{1}{2}-i\frac{q\mu_0}{6},\nu_{k_\ell}}(2i\frac{x}{6}) + \frac{i(-1)^\alpha k_\ell}{\sqrt{6}} W_{-\frac{1}{2}-i\frac{q\mu_0}{6},\nu_{k_\ell}}(2i\frac{x}{6})\Big] \end{pmatrix} \tag{4.14}$$

where $\nu_{k_\ell} = \sqrt{\frac{k_\ell^2}{6} - q^2(\frac{\mu_0}{6})^2}$ and $c_{(\alpha,\text{in})}, c_{(\alpha,\text{out})}$ are arbitrary constants.

In the coordinate x the horizon is located at $x \to \infty$ and the matching region is at $x \to 0$. Imposing the infalling boundary condition for $\Phi^{(0,\ell)}_\alpha$ near the horizon, in the matching region we find the following analytic solution for $\Phi^{(0,\ell)}_\alpha$:

$$\Phi^{(0,\ell)}_\alpha = v^{(0,\ell)}_{-\alpha}\big(\frac{1}{r-1}\big)^{-\nu_{k_\ell}} + v^{(0,\ell)}_{+\alpha}\mathcal{G}^{(0,\ell)}_{\alpha\text{IR}}(\omega)\big(\frac{1}{r-1}\big)^{\nu_{k_\ell}} + \dots \tag{4.15}$$

where we have chosen the normalizalition of the leading coefficient to equal

$$v^{(0,\ell)}_{\pm\alpha} = \tilde{c}_0 \begin{pmatrix} \pm\nu_{k_\ell} \\ \frac{q\mu_0}{6} - (-1)^\alpha \frac{k_\ell}{\sqrt{6}} \end{pmatrix}. \tag{4.16}$$

This determines the "pure AdS IR Green's function" to be

$$\mathcal{G}^{(0,\ell)}_{\alpha\text{IR}}(\omega) = e^{-i\pi\nu_{k_\ell}} \frac{\Gamma(-2\nu_{k_\ell})\Gamma(1+\nu_{k_\ell}-\frac{i\mu_0 q}{6})((-1)^\alpha i\sqrt{6}k_\ell - 6\nu_{k_\ell} - i\mu_0 q)}{\Gamma(2\nu_{k_\ell})\Gamma(1-\nu_{k_\ell}-\frac{i\mu_0 q}{6})((-1)^\alpha i\sqrt{6}k_\ell + 6\nu_{k_\ell} - i\mu_0 q)} \big(\frac{\omega}{3}\big)^{2\nu_{k_\ell}}. \tag{4.17}$$

It will be useful to introduce a shorthand for the prefactor $\mathcal{G}^{(0,\ell)}_{\alpha\text{IR}}(\omega) = \tilde{\mathcal{G}}^\ell_{\alpha\text{IR}}\omega^{2\nu_{k_\ell}}$.

4.2.2 Near region solutions for $\Phi^{(1,\ell)}_\alpha$

We now consider the near region solutions for $\Phi^{(1,\ell)}_\alpha$. The equation of motion for $\Phi^{(1,\ell)}_\alpha$ in the near region reduces to

$$\begin{aligned}\partial_r\Phi^{(1,\ell)}_\alpha - \frac{i}{6(r-1)^2}(\omega + q\mu_0(r-1))\sigma^2\Phi^{(1,\ell)}_\alpha - (-1)^\alpha\frac{1}{\sqrt{6}(r-1)}k_\ell\sigma^1\Phi^{(1,\ell)}_\alpha \\ - iq\sigma^2\frac{1}{6(r-1)}\sum_{\beta;\ell'=\ell\pm1} M_{\alpha\beta,\ell\ell'}\Phi^{(0,\ell')}_\beta = 0.\end{aligned} \tag{4.18}$$

Similar to the $\Phi^{(0,\ell)}_\alpha$ case, we perform a coordinate transformation $x = \frac{\omega}{r-1}$ and obtain

$$\partial_x^2\Phi^{(1,\ell)}_{\alpha j} + (\frac{2}{x} - \frac{\partial_x h_{\alpha j}}{h_{\alpha j}})\partial_x\Phi^{(1,\ell)}_{\alpha j} + \frac{h_{\alpha 1}h_{\alpha 2}}{x^4}\Phi^{(1,\ell)}_{\alpha j} + \frac{1}{x^4}X^\ell_{\alpha j} = 0, \tag{4.19}$$

with $h_{\alpha j}$ as before (see eq. (4.12)) and

$$\begin{aligned} X^\ell_{\alpha j} &= \sum_{\beta;\ell'=\ell\pm1} X^\ell_{(\alpha j,\beta\ell')}, \\ X^\ell_{(\alpha j,\beta\ell')} &\equiv -\frac{qh_{\alpha j}x}{6}M_{\alpha\beta,\ell\ell'}\Phi^{(0,\ell')}_{\beta j} - (-1)^j x^2 h_{\alpha j}\partial_x\Big[\frac{qx}{6h_{\alpha j}}M_{\alpha\beta,\ell\ell'}\Phi^{(0,\ell')}_{\beta l}\Big] \end{aligned} \tag{4.20}$$

with $\Phi^{(0,\ell)}_{\alpha j}$ being the zeroth order solution and $l = 3 - j$.

We know that the solutions of inhomogeneous equations can be derived from the solutions of the corresponding homogeneous equations. Let us denote the two linear independent solutions of the $\alpha\ell, j$-th homogeneous equation as ${\eta_1}^{\ell}_{\alpha j}$ and ${\eta_2}^{\ell}_{\alpha j}$. Specifically we shall choose ${\eta_1}^{\ell}_{\alpha j} = \Phi^{(0,\ell),\text{in}}_{\alpha}$ to be the infalling solution and ${\eta_2}^{\ell}_{\alpha j} = \Phi^{(0,\ell),\text{out}}_{\alpha}$ to be the outgoing solution given in eqns (4.13) and (4.14). Then the special solution ${\eta_s}^{\ell}_{\alpha j}$ to the inhomogeneous equations (4.19) is obtained using the standard Green's function

$$G^{\ell}_{\alpha j}(x, x') = \frac{{\eta_1}^{\ell}_{\alpha j}(x){\eta_2}^{\ell}_{\alpha j}(x')\theta(x - x') + {\eta_1}^{\ell}_{\alpha j}(x'){\eta_2}^{\ell}_{\alpha j}(x)\theta(x' - x)}{W(x)} \tag{4.21}$$

where $W(x)$ is the Wronskian of the system $W(x) = {\eta_1}^{\ell}_{\alpha j}\partial_x{\eta_2}^{\ell}_{\alpha j} - {\eta_2}^{\ell}_{\alpha j}\partial_x{\eta_1}^{\ell}_{\alpha j}$; it is proportional to $W(x) = g_0\frac{h_{\alpha j}}{x^2}$ with g_0 a constant independent of x. We find (recall that $x \in [0, \infty)$)

$${\eta_{s,\text{canonical}}}^{(1,\ell)}_{(\alpha j,\beta\ell')}(x) = {\eta_1}^{\ell}_{\alpha j}(x)\int_0^x dx' \frac{{\eta_2}^{\ell}_{\alpha j}X^{\ell}_{(\alpha j,\beta\ell')}}{x'^4 W(x')} + {\eta_2}^{\ell}_{\alpha j}(x)\int_x^{\infty} dx' \frac{{\eta_1}^{\ell}_{\alpha j}X^{\ell}_{(\alpha j,\beta\ell')}}{x'^4 W(x')} \tag{4.22}$$

Note that we have restricted the solution to only one of the source terms in (4.20). This is a consequence of the boundary conditions we choose: for a specific $\alpha\ell$-th b.c., only one zeroth order field is non-vanishing.

The special solution for a second order inhomogeneous equation is not unique, however. Different special solutions can differ by additional homogeneous contributions $c_1\eta_1 + c_2\eta_2$, where c_1 and c_2 are arbitrary constants. The coefficients in front of the outgoing homogeneous solutions must be fixed by the boundary conditions, while the coefficients in front of the ingoing homogeneous solutions will not affect the final result. Note that this degree of freedom can be absorded by changing the fixed limits of the integrations in (4.22): special solutions obtained with different limits of integrations differ precisely by homogenous terms.

Here we are instructed to choose the infalling boundary condition at the horizon, $x = \infty$. Since ${\eta_1}^{\ell}_{\alpha j}$ is the homogeneous infalling solution, it is easily seen that this fixes the upper limit of the second integration in (4.22) term to be ∞. For convenience we choose the *undetermined* limit of the first integration term to also be located at the horizon. This change simply means that the special solution we shall work with is

$${\eta_s}^{(1,\ell)}_{(\alpha j,\beta\ell')}(x) = -{\eta_1}^{\ell}_{\alpha j}(x)\int_x^{\infty} dx' \frac{{\eta_2}^{\ell}_{\alpha j}X^{\ell}_{(\alpha j,\beta\ell')}}{x'^4 W(x')} + {\eta_2}^{\ell}_{\alpha j}(x)\int_x^{\infty} dx' \frac{{\eta_1}^{\ell}_{\alpha j}X^{\ell}_{(\alpha j,\beta\ell')}}{x'^4 W(x')}. \tag{4.23}$$

Thus the most general solution with the infalling boundary condition in the near region is

$$\Phi^{(1,\ell)}_{\alpha j}(x) = {\eta_s}^{(1,\ell)}_{\alpha j}(x) + c_4{\eta_1}^{(\ell)}_{\alpha j}(x), \tag{4.24}$$

where c_4 is an arbitrary constant. The choice of c_4 just corresponds to changing the *normalization* of the infalling boundary conditions of the homogeneous solution at first

order in ϵ. Since the final Green's functions (or spectral functions) do not depend on the normalization, we may freely set $c_4 = 0$.

Now we need to see how this infalling special solution behaves at the boundary of the near region $x \ll 1$ in order to match it to the far region. To do so, we split the integration into two parts

$$\begin{aligned}\eta_{s\,(\alpha j,\beta\ell')}^{(1,\ell)}(x) = &-\eta_{1\,\alpha j}^{\ell}\int_{\varepsilon}^{\infty} dx' \frac{\eta_{2\,\alpha j}^{\ell} X_{(\alpha j,\beta\ell')}^{\ell}}{x'^4 W(x')} + \eta_{2\,\alpha j}^{\ell}\int_{\varepsilon}^{\infty} dx' \frac{\eta_{2\,\alpha j}^{\ell} X_{(\alpha j,\beta\ell')}^{\ell}}{x'^4 W(x')} \\ &-\eta_{1\,\alpha j}^{\ell}\int_{x}^{\varepsilon} dx' \frac{\eta_{2\,\alpha j}^{\ell} X_{(\alpha j,\beta\ell')}^{\ell}}{x'^4 W(x')} + \eta_{2\,\alpha j}^{\ell}\int_{x}^{\varepsilon} dx' \frac{\eta_{1\,\alpha j}^{\ell} X_{(\alpha j,\beta\ell')}^{\ell}}{x'^4 W(x')},\end{aligned} \tag{4.25}$$

where ε is a very small but nonzero constant parameter. Because ε is a constant, $\int_{\varepsilon}^{\infty} dx \frac{\eta_{i\,\alpha j}^{\ell} X_{(\alpha j,\beta\ell')}^{\ell}}{x^4 W(x)}$, $i = 1, 2$ are also constants. Thus the x-dependence of first two terms in (4.25) is direcly determined by the x-dependence of the homogeneous solutions $\eta_{i\,\alpha j}^{\ell}(x)$.

In the second part, if both x and ε are very small, we can replace the integrands by their asymptotic values. For $\omega \ll r - 1$ these asymptotic values are (see (4.15))

$$\eta_{1\alpha j} \sim \omega^{\nu_{k_\ell}}\left(x^{-\nu_{k_\ell}} + \tilde{\mathcal{G}}_{IR} x^{\nu_{k_\ell}}\right), \quad \eta_{2\alpha j} \sim \omega^{\nu_{k_\ell}}\left(x^{-\nu_{k_\ell}} + \tilde{\mathcal{G}}_{IR}^{\dagger} x^{\nu_{k_\ell}}\right).$$

The convenient way to substitute this into (4.25) is to note that our choice of the special solution (4.23) has been made such that under a linear transformation to a different basis of the homogeneous equations

$$\eta_{1\alpha j} = a_{1\alpha j}\tilde{\eta}_{1\alpha j} + a_{2\alpha j}\tilde{\eta}_{2\alpha j}, \quad \eta_{2\alpha j} = b_{1\alpha j}\tilde{\eta}_{1\alpha j} + b_{2\alpha j}\tilde{\eta}_{2\alpha j}, \tag{4.26}$$

the special solution is invariant. Choosing $\tilde{\eta}_{1\alpha j}$ to be the two independent scaling solutions

$$\tilde{\eta}_{1\alpha j} \sim x^{-\nu_{k_\ell}}, \quad \tilde{\eta}_{2\alpha j} \sim x^{\nu_{k_\ell}}, \quad \text{when } x \to 0, \tag{4.27}$$

it is now straightforward to extract the leading ω-dependence of $\Phi^{(1,\ell)}$. All dependence on the frequency ω is contained in $x = \frac{\omega}{r-1}$ plus the explicit factors $\omega^{2\nu_{k_\ell}}$ in $\tilde{\eta}_{i\alpha j}^{(0,\ell)}$. One readily obtains (when $x \to 0$)

$$\begin{aligned}\eta_{s\,(\alpha j,\beta\ell')}^{(1,\ell)} \simeq\ & x^{\nu_{k_\ell}}\omega^{\nu_{k_{\ell'}}} n_{1\,\alpha j\beta\ell'}^{\ell} + x^{-\nu_{k_\ell}}\omega^{\nu_{k_{\ell'}}} n_{2\,\alpha j\beta\ell'}^{\ell} \\ &+ x^{\nu_{k_{\ell'}}}\omega^{\nu_{k_{\ell'}}} n_{3\,\alpha j\beta\ell'}^{\ell} + x^{-\nu_{k_{\ell'}}}\omega^{\nu_{k_{\ell'}}} n_{4\,\alpha j\beta\ell'}^{\ell} + \ldots\end{aligned} \tag{4.28}$$

where the coefficients n_i $(i = 1, ..., 4)$ do not depend on ω or x. The explicit solutions to ${\eta_s^{(1,\ell)}}_{\alpha j,\beta\ell'}$ are given in the appendix (A.1).

The next step is more subtle. Note, firstly, that the normalization with an explicit $\omega^{\nu_{k_\ell}}$ chosen in (4.26) is convenient as the function $\Phi^{(0,\ell)}(r)$ is then manifestly analytic around $\omega = 0$. The special solution (4.28) scales to leading order as $\omega^{\nu_{k_{\ell'}}+\nu_{k_\ell}}$, $\omega^{\nu_{k_{\ell'}}-\nu_{k_\ell}}$, $\omega^{2\nu_{k_{\ell'}}}$ or ω^0 respectively. This is not analytic if $\nu_{k_{\ell'}} - \nu_{k_\ell} < 0$. However, this cannot be corrected

by chosing a new normalization: for the special solution (4.28) the normalization is *not* free. We can, however, eliminate this divergence using the freedom to add a homogeneous solution, i.e. the actual solution

$$\Phi^{(1,\ell)}_{\alpha j,\beta\ell'}(x) = \eta_s{}^{(1,\ell)}_{\alpha j,\beta\ell'}(x) + c_4\eta^{(0,\ell)}_{\alpha j}(x) \tag{4.29}$$

with c_4 a function of ω chosen such that $\Phi^{(1,\ell)}_{\alpha j,\beta\ell'}(x)$ is analytic in ω. Recall that $\eta^{(0,\ell)}_{\alpha j} = (x^{-\nu_{k_\ell}} + \tilde{\mathcal{G}}_{IR}x^{\nu_{k_\ell}}) + \ldots$. This is therefore the case if

$$c_4 = -\omega^{\nu_{k_{\ell'}}} n_2{}^{\ell}_{\alpha j\beta\ell'}. \tag{4.30}$$

Though the insistence on analyticity in ω may appear arbitrary, it is clear that this is the only sensible solution to be able to use the matching method with the far region $\frac{\omega}{r-1} \ll 1$. Doing so, one finds that the first-order solution near $x \to 0$ equals

$$\begin{aligned}\Phi^{(1,\ell)}_{(\alpha j,\beta\ell')} &\simeq x^{\nu_{k_\ell}}\omega^{\nu_{k_{\ell'}}}\tilde{n_1}{}^{\ell}_{\alpha j\beta\ell'} + x^{\nu_{k_{\ell'}}}\omega^{\nu_{k_{\ell'}}} n_3{}^{\ell}_{\alpha j\beta\ell'} + x^{-\nu_{k_{\ell'}}}\omega^{\nu_{k_{\ell'}}} n_4{}^{\ell}_{\alpha j\beta\ell'} \\ &\simeq \big(\frac{1}{r-1}\big)^{\nu_{k_\ell}}\omega^{\nu_{k_\ell}+\nu_{k_{\ell'}}}\tilde{n_1}{}^{\ell}_{\alpha j\beta\ell'} + \big(\frac{1}{r-1}\big)^{\nu_{k_{\ell'}}}\omega^{2\nu_{k_{\ell'}}} n_3{}^{\ell}_{\alpha j\beta\ell'} + \big(\frac{1}{r-1}\big)^{-\nu_{k_{\ell'}}} n_4{}^{\ell}_{\alpha j\beta\ell'},\end{aligned} \tag{4.31}$$

where

$$\tilde{n_1}{}^{\ell}_{\alpha j\beta\ell'} = \left(n_1{}^{\ell}_{\alpha j\beta\ell'} - (-1)^j\tilde{\mathcal{G}}^{(0,\ell)}_{\mathrm{IR}\alpha} n_2{}^{\ell}_{\alpha j\beta\ell'}\right) \tag{4.32}$$

and in the second line we have substituted $x = \frac{\omega}{r-1}$.

The solution above is for general momenta, but it is not valid in the degenerate case when $\nu_{k_\ell} = \nu_{k_{\ell'}}$. This condition precisely gives the two points on the boundary of the first Brillouin zone (see Fig. 2). Thus we encounter here the similar situation to what happens in the standard band structure in condensed matter physics. At the first Brillouin boundary, $k_x = \pm\frac{K}{2}$,the modes with $\ell = 0$ are degenerate with modes $\ell = \mp 1$. We will discuss the physics at this special boundary in more detail in the subsection 4.2.4 after we construct the second order non-degenerate near horizon solution.

4.2.3 Near region solutions for $\Phi^{(2,\ell)}_{\alpha}$

Finally, as we argued above eq. (4.9) we also need the second order solution $\Phi^{(2,\ell)}_{\alpha}$. Its equation of motion in the near horizon region is

$$\begin{aligned}&\partial_r\Phi^{(2,\ell)}_{\alpha} - \frac{i}{6(r-1)^2}(\omega + q\mu_0(r-1))\sigma^2\Phi^{(2,\ell)}_{\alpha} - (-1)^{\alpha}\frac{1}{\sqrt{6}(r-1)}k_\ell\sigma^1\Phi^{(2,\ell)}_{\alpha} \\ &\quad - iq\sigma^2\frac{1}{6(r-1)}\sum_{\beta;\ell'=\ell\pm1} M_{\alpha\beta,\ell\ell'}\Phi^{(1,\ell')}_{\beta} = 0.\end{aligned} \tag{4.33}$$

Transforming to the coordinate $x = \frac{\omega}{r-1}$ again, we find

$$\partial_x^2\Phi^{(2,\ell)}_{\alpha j} + \big(\frac{2}{x} - \frac{\partial_x h_{\alpha j}}{h_{\alpha j}}\big)\partial_x\Phi^{(2,\ell)}_{\alpha j} + \frac{h_{\alpha 1}h_{\alpha 2}}{x^4}\Phi^{(2,\ell)}_{\alpha j} + \frac{1}{x^4}Y^{\ell}_{\alpha j} = 0, \tag{4.34}$$

with $h_{\alpha j}$ as before in eq. (4.12). The inhomogenous term now equals

$$Y^{\ell}_{\alpha j} = -\frac{q h_{\alpha j} x}{6} \sum_{\beta;\ell'=\ell\pm1} M_{\alpha\beta,\ell\ell'} \Phi^{(1,\ell')}_{\beta j} - (-1)^j x^2 \sum_{\beta;\ell'=\ell\pm1} \partial_x \left[\frac{qx}{6h_{\alpha j}} M_{\alpha\beta,\ell\ell'} \Phi^{(1,\ell')}_{\beta l} \right] h_{\alpha j} \quad (4.35)$$

with $l = 3-j$. In contrast to the first order case, both components in the $\ell \pm 1$ sectors will now contribute.

Through the Green's function (4.21), the special solution can be written as:

$$\eta_{s\,(\alpha j)}^{(2,\ell)}(x) = -\eta_{1\alpha j}^{\ell}(x) \int_x^{\infty} dx' \frac{\eta_{2\alpha j}^{\ell} Y^{\ell}_{\alpha j}}{x'^4 W(x')} + \eta_{2\alpha j}^{\ell}(x) \int_x^{\infty} dx' \frac{\eta_{1\alpha j}^{\ell} Y^{\ell}_{\alpha j}}{x'^4 W(x')}. \quad (4.36)$$

It is an infalling solution as long as the upper bound of the integration in the second term is ∞. Using the method similar to last subsection, one can obtain the behavior of the special solution near $x = 0$:

$$\begin{aligned} \eta_{s\,(\alpha j)}^{(2,\ell)} \simeq\ & x^{\nu_{k_\ell}} \omega^{\nu_{k_\ell}} s_{1\alpha j}^{\ell} + x^{-\nu_{k_\ell}} \omega^{\nu_{k_\ell}} s_{2\alpha j}^{\ell} + \sum_{\ell'=\ell\pm1} \left(x^{\nu_{k_{\ell'}}} \omega^{\nu_{k_\ell}} s_{3\alpha j\ell'}^{\ell} \right) \\ & + x^{\nu_{k_\ell}} \omega^{\nu_{k_\ell}} \ln(\frac{1}{r-1}) s_{4\alpha j}^{\ell} + x^{-\nu_{k_\ell}} \omega^{\nu_{k_\ell}} \ln(\frac{1}{r-1}) s_{5\alpha j}^{\ell} + x^{\nu_{k_\ell}} \omega^{\nu_{k_\ell}} (\ln\omega) s_{4\alpha j}^{\ell} \\ & + x^{-\nu_{k_\ell}} \omega^{\nu_{k_\ell}} (\ln\omega) s_{5\alpha j}^{\ell} + \dots \end{aligned} \quad (4.37)$$

where the coefficients $s_{i\alpha j}^{\ell}$ do not depend on x or ω and the concrete expressions can be found in (A.3). Note again the degeneracy at $\nu_{k_\ell} = \nu_{k_{\ell'}}$.

Similar to the first order case, the special solution is not regular in the $\omega \to 0$ limit. Making use of the freedom of adding arbitrary infalling solutions, one can obtain the regular second order solution:

$$\begin{aligned} \Phi_{(\alpha j)}^{(2,\ell)} \simeq\ & x^{\nu_{k_\ell}} \omega^{\nu_{k_\ell}} \tilde{s}_{1\alpha j}^{\ell} + \sum_{\ell'=\ell\pm1} \left(x^{\nu_{k_{\ell'}}} \omega^{\nu_{k_\ell}} s_{3\alpha j\ell'}^{\ell} \right) + x^{\nu_{k_\ell}} \omega^{\nu_{k_\ell}} \ln(\frac{1}{r-1}) s_{4\alpha j}^{\ell} \\ & + x^{-\nu_{k_\ell}} \omega^{\nu_{k_\ell}} \ln(\frac{1}{r-1}) s_{5\alpha j}^{\ell} + x^{\nu_{k_\ell}} \omega^{\nu_{k_\ell}} (\ln\omega) \tilde{s}_{4\alpha j}^{\ell} + \dots . \end{aligned} \quad (4.38)$$

Substituting $x = \frac{\omega}{r-1}$ to display the explicit leading dependence on ω we find

$$\begin{aligned} \Phi_{(\alpha j)}^{(2,\ell)} \simeq\ & \left(\frac{1}{r-1}\right)^{\nu_{k_\ell}} \omega^{2\nu_{k_\ell}} \tilde{s}_{1\alpha j}^{\ell} + \sum_{\ell'=\ell\pm1} \left[\left(\frac{1}{r-1}\right)^{\nu_{k_{\ell'}}} \omega^{\nu_{k_{\ell'}}+\nu_{k_\ell}} s_{3\alpha j\ell'}^{\ell} \right] \\ & + \left(\frac{1}{r-1}\right)^{\nu_{k_\ell}} \omega^{2\nu_{k_\ell}} \ln(\frac{1}{r-1}) s_{4\alpha j}^{\ell} + \left(\frac{1}{r-1}\right)^{-\nu_{k_\ell}} \ln(\frac{1}{r-1}) s_{5\alpha j}^{\ell} \\ & + \left(\frac{1}{r-1}\right)^{\nu_{k_\ell}} \omega^{2\nu_{k_\ell}} (\ln\omega) \tilde{s}_{4\alpha j}^{\ell} + \dots \end{aligned} \quad (4.39)$$

where

$$\tilde{s}_{1\alpha j}^{\ell} = s_{1\alpha j}^{\ell} - (-1)^j s_{2\alpha j}^{\ell} \tilde{\mathcal{G}}_{\alpha}^{\ell}, \quad \tilde{s}_{4\alpha j}^{\ell} = s_{4\alpha j}^{\ell} - (-1)^j s_{5\alpha j}^{\ell} \tilde{\mathcal{G}}_{\alpha}^{\ell}. \quad (4.40)$$

4.2.4 Near region solutions for the Degenerate case $\nu_{k_\ell} = \nu_{k_{\ell'}}$

As pointed out in the previous subsections, a degeneracy occurs whenever $\nu_{k_\ell} = \nu_{k_{\ell'}}$ where $\ell' = \ell \pm 1$ and this case must be treated in more detail. This degeneracy happens at the edges of the Brillioun zones when $k_x = \frac{1}{2a}$, $\ell = 0, -1$ and $k_x = -\frac{1}{2a}$, $\ell = 0, 1$ for any fixed k_y (see Fig. 2).

Specifically what goes wrong when $\nu_{k_\ell} = \nu_{k_{\ell'}}$ is that the coefficients $n^{\ell}_{i_{\alpha j}}$ in (4.31) (explicitly given in (A.1)) and $s^{\ell}_{i_{\alpha j}}$ in eq. (4.39) (explicitly given in eq.(A.3)) become divergent. The solutions we obtain in this section can be seen as the continuous $\nu \to \nu'$ limit of the near-horizon solutions in previous two subsections. However, in the next subsection where we address far region solutions, we will see that at the boundary the degenerate case is qualitatively quite different.

Repeating the procedure in the previous subsections, for this special case $\nu_{k_{\ell'}} = \nu_{k_\ell}$, we can obtain the leading ω-behavior of the infalling first order degenerate special solution near the matching point as

$$\begin{aligned}\eta_s{}^{(1,\ell)}_{(\alpha j,\beta\ell')} \simeq\ & x^{\nu_{k_\ell}}\omega^{\nu_{k_\ell}} d_1{}^{\ell}_{\alpha j\beta\ell'} + x^{-\nu_{k_\ell}}\omega^{\nu_{k_\ell}} d_2{}^{\ell}_{\alpha j\beta\ell'} + x^{\nu_{k_\ell}}\omega^{\nu_{k_\ell}}(\ln\omega) d_3{}^{\ell}_{\alpha j\beta\ell'} + x^{-\nu_{k_\ell}}\omega^{\nu_{k_\ell}}(\ln\omega) d_4{}^{\ell}_{\alpha j\beta\ell'} \\ & + x^{\nu_{k_\ell}}\omega^{\nu_{k_\ell}} d_3{}^{\ell}_{\alpha j\beta\ell'} \ln\frac{1}{r-1} + x^{-\nu_{k_\ell}}\omega^{\nu_{k_\ell}} d_4{}^{\ell}_{\alpha j\beta\ell'} \ln\frac{1}{r-1} + \dots \end{aligned} \tag{4.41}$$

where the coefficients $d^{\ell}_{i_{\alpha j\beta\ell'}}$ do not depend on ω or x and their expressions can be found in the appendix, eq. (A.5). Removing the potential divergence in ω as $\omega \to 0$, related to the term $x^{-\nu_{k_\ell}}\omega^{\nu_{k_\ell}} \ln\omega$ by adding a zeroth order infalling solution, we find:

$$\begin{aligned}\Phi_{\text{degen}}{}^{(1,\ell)}_{(\alpha j,\beta\ell')} \simeq\ & \left(\frac{1}{r-1}\right)^{\nu_{k_\ell}} \omega^{2\nu_{k_\ell}} \tilde{d}_1{}^{\ell}_{\alpha j\beta\ell'} + 2\left(\frac{1}{r-1}\right)^{\nu_{k_\ell}} \omega^{2\nu_{k_\ell}}(\ln\omega) d^{\ell}_{3\alpha j\beta\ell'} \\ & + \left(\frac{1}{r-1}\right)^{\nu_{k_\ell}} \omega^{2\nu_{k_\ell}} d^{\ell}_{3\alpha j\beta\ell'} \ln\frac{1}{r-1} + \left(\frac{1}{r-1}\right)^{-\nu_{k_\ell}} d^{\ell}_{4\alpha j\beta\ell'} \ln\frac{1}{r-1} + \dots \end{aligned} \tag{4.42}$$

where

$$\tilde{d}_1{}^{\ell}_{\alpha j\beta\ell'} = d_1{}^{\ell}_{\alpha j\beta\ell'} - (-1)^j d_{2\alpha j\beta\ell'} \tilde{\mathcal{G}}^{\ell}_{\alpha}. \tag{4.43}$$

The statement that this is the continous limit from the non-degenerate case is that the novel logarithmic term originates in from the combination $\frac{\omega^{\nu+\nu'} - \omega^{2\nu'}}{\nu - \nu'}$. It is precisely this combination that arises when we subsitute in the exact values of the coefficients $n^{\ell}_{i_{\alpha j\beta\ell'}}$.

We similarly obtain the infalling second order special solution near the matching point. As pointed out in Sec. 4.2.3 , both $\Phi^{(1,\ell\pm1)}$ source terms contribute to second order special solution. Only one of them can at any one time be degenerate in the sense that $\nu_{k_\ell} = \nu_{k_{\ell'}}$ with $\ell' = \ell + 1$ or $\ell' = \ell - 1$. Following the same steps as before, the leading ω-behavior of

the infalling second order degenerate solution behaves near the matching point as:

$$\begin{aligned}\eta_{s\,(\alpha j,\ell')}^{(2,\ell)} \simeq\ & x^{\nu_{k_\ell}}\omega^{\nu_{k_\ell}}\mathtt{s}_{1\,\alpha j\ell'}^{\ell}+x^{-\nu_{k_\ell}}\omega^{\nu_{k_\ell}}\mathtt{s}_{2\,\alpha j\ell'}^{\ell}+x^{\nu_{k_\ell}}\omega^{\nu_{k_\ell}}\mathtt{s}_{3\,\alpha j\ell'}^{\ell}\ln\omega+x^{-\nu_{k_\ell}}\omega^{\nu_{k_\ell}}\mathtt{s}_{4\,\alpha j\ell'}^{\ell}\ln\omega\\ &+x^{\nu_{k_\ell}}\omega^{\nu_{k_\ell}}\mathtt{s}_{5\,\alpha j\ell'}^{\ell}\ln\frac{1}{r-1}+x^{-\nu_{k_\ell}}\omega^{\nu_{k_\ell}}\mathtt{s}_{6\,\alpha j\ell'}^{\ell}\ln\frac{1}{r-1}+x^{\nu_{k_\ell}}\omega^{\nu_{k_\ell}}\mathtt{s}_{7\,\alpha j\ell'}^{\ell}\ln\omega\ln\frac{1}{r-1}\\ &+x^{\nu_{k_\ell}}\omega^{\nu_{k_\ell}}\mathtt{s}_{8\,\alpha j\ell'}^{\ell}(\ln\omega)^2+x^{-\nu_{k_\ell}}\omega^{\nu_{k_\ell}}\mathtt{s}_{9\,\alpha j\ell'}^{\ell}(\ln\omega)^2\\ &+x^{\nu_{k_\ell}}\omega^{\nu_{k_\ell}}\mathtt{s}_{10\,\alpha j\ell'}^{\ell}(\ln\frac{1}{r-1})^2+x^{-\nu_{k_\ell}}\omega^{\nu_{k_\ell}}\mathtt{s}_{11\,\alpha j\ell'}^{\ell}(\ln\frac{1}{r-1})^2+\dots.\end{aligned}\tag{4.44}$$

The explicit expressions for the ω, x-independent coefficients $\mathtt{s}_{i\,\alpha j\ell'}^{\ell}$ are given in (A.6). The $\omega\to 0$-regular second order degenerate solution is:

$$\begin{aligned}\Phi_{\text{degen}\,(\alpha j,\ell')}^{(2,\ell)} \simeq\ & \left(\frac{1}{r-1}\right)^{\nu_{k_\ell}}\omega^{2\nu_{k_\ell}}\tilde{\mathtt{s}}_{1\,\alpha j\ell'}^{\ell}+\left(\frac{1}{r-1}\right)^{\nu_{k_\ell}}\omega^{2\nu_{k_\ell}}\ln\omega\tilde{\mathtt{s}}_{3\,\alpha j\ell'}^{\ell}+\left(\frac{1}{r-1}\right)^{\nu_{k_\ell}}\omega^{2\nu_{k_\ell}}\mathtt{s}_{5\,\alpha j\ell'}^{\ell}\ln\frac{1}{r-1}\\ &+\left(\frac{1}{r-1}\right)^{-\nu_{k_\ell}}\mathtt{s}_{6\,\alpha j\ell'}^{\ell}\ln\frac{1}{r-1}+\left(\frac{1}{r-1}\right)^{\nu_{k_\ell}}\omega^{2\nu_{k_\ell}}\ln\omega\mathtt{s}_{7\,\alpha j\ell'}^{\ell}\ln\frac{1}{r-1}\\ &+\left(\frac{1}{r-1}\right)^{\nu_{k_\ell}}\omega^{2\nu_{k_\ell}}(\ln\omega)^2\tilde{\mathtt{s}}_{8\,\alpha j\ell'}^{\ell}+\left(\frac{1}{r-1}\right)^{\nu_{k_\ell}}\omega^{2\nu_{k_\ell}}\mathtt{s}_{10\,\alpha j\ell'}^{\ell}(\ln\frac{1}{r-1})^2\\ &+\left(\frac{1}{r-1}\right)^{-\nu_{k_\ell}}\mathtt{s}_{11\,\alpha j\ell'}^{\ell}(\ln\frac{1}{r-1})^2\end{aligned}\tag{4.45}$$

where

$$\tilde{\mathtt{s}}_{1\,\alpha j}^{\ell}=\mathtt{s}_{1\,\alpha j}^{\ell}-(-1)^j\mathtt{s}_{2\,\alpha j}^{\ell}\tilde{\mathcal{G}}_{\alpha}^{\ell},\quad \tilde{\mathtt{s}}_{3\,\alpha j}^{\ell}=\mathtt{s}_{3\,\alpha j}^{\ell}-(-1)^j\mathtt{s}_{4\,\alpha j}^{\ell}\tilde{\mathcal{G}}_{\alpha}^{\ell},\quad \tilde{\mathtt{s}}_{8\,\alpha j}^{\ell}=\mathtt{s}_{8\,\alpha j}^{\ell}-(-1)^j\mathtt{s}_{9\,\alpha j}^{\ell}\tilde{\mathcal{G}}_{\alpha}^{\ell}.\tag{4.46}$$

4.2.5 The far region

From the original equation of motion (4.2) it is immediately clear that in the far region, $r-1\gg\omega$, the terms in the equations of motion containing ω are automatically subleading in $\frac{1}{r-1}$. The $1/(r-1)$ expansion is therefore correlated with an expansion in the frequency ω. The leading, ω-independent, order equation of motion for $\Phi_{\alpha}^{(0,\ell)}$ in the far region equals

$$(\partial_r+m\sqrt{g_{rr}}\sigma^3)\Phi_{\alpha}^{(0,\ell)}-i\sqrt{\frac{g_{rr}}{g_{tt}}}(q\mu_0(1-\frac{1}{r}))\sigma^2\Phi_{\alpha}^{(0,\ell)}-(-1)^{\alpha}\sqrt{\frac{g_{rr}}{g_{xx}}}k_\ell\sigma^1\Phi_{\alpha}^{(0,\ell)}=0,\tag{4.47}$$

the leading order far region equation of motion for $\Phi_{\alpha}^{(1,\ell)}$ equals

$$\begin{aligned}&(\partial_r+m\sqrt{g_{rr}}\sigma^3)\Phi_{\alpha}^{(1,\ell)}-i\sqrt{\frac{g_{rr}}{g_{tt}}}(q\mu_0(1-\frac{1}{r}))\sigma^2\Phi_{\alpha}^{(1,\ell)}-(-1)^{\alpha}\sqrt{\frac{g_{rr}}{g_{xx}}}k_\ell\sigma^1\Phi_{\alpha}^{(1,\ell)}\\ &-iq\sqrt{\frac{g_{rr}}{g_{tt}}}\sigma^2(1-\frac{1}{r})\sum_{\beta;\ell'=\ell\pm1}M_{\alpha\beta,\ell\ell'}\Phi_{\beta}^{(0,\ell')}=0,\end{aligned}\tag{4.48}$$

and the leading order far region equation of motion for $\Phi_{\alpha}^{(2,\ell)}$ is similar. Recalling that $\sqrt{g_{rr}}\sim 1/\sqrt{g_{tt}}\sim 1/\sqrt{g_{xx}}\sim 1/r$ we see that at the boundary of the AdS spacetime $r\to\infty$,

the equations for all orders in the modulation ϵ linearize and all fields $\Phi_\alpha^{(s)}$ for any order behave as

$$\Phi_\alpha^{(s,\ell)} = A_\alpha^{(s,\ell)} r^m \begin{pmatrix} 0 \\ 1 \end{pmatrix} + B_\alpha^{(s,\ell)} r^{-m} \begin{pmatrix} 1 \\ 0 \end{pmatrix} + \dots, \qquad s = 0, 1, 2.... \tag{4.49}$$

The coefficients $A_\alpha^{(s,\ell)}$ and $B_\alpha^{(s,\ell)}$ are determined by matching these solutions at the inner boundary of the far region with the $x \to 0$ value of the near horizon infalling solutions obtained in the previous subsections: Eqs (4.15), (4.31) and (4.39) or (4.42) and (4.45). The equation of the zeroth order field $\Phi_\alpha^{(0,\ell)}(r)$ is homogenous and linear, so under the near horizon $\alpha\ell$-th boundary condition the boundary value of the zeroth order solution can be obtained using the matching method to be

$$A_\alpha^{(0,\ell)} = A^{(0)-}_{\alpha\ell,\alpha\ell} v^{(0,\ell)}_{-\alpha 2} + \mathcal{G}^{(0,\ell)}_{\alpha \mathrm{IR}} A^{(0)+}_{\alpha\ell,\alpha\ell} v^{(0,\ell)}_{+\alpha 2}, \quad B_\alpha^{(0,\ell)} = B^{(0)-}_{\alpha\ell,\alpha\ell} v^{(0,\ell)}_{-\alpha 1} + \mathcal{G}^{(0,\ell)}_{\alpha \mathrm{IR}} B^{(0)+}_{\alpha\ell,\alpha\ell} v^{(0,\ell)}_{+\alpha 1} \tag{4.50}$$

where $A^{(0)\pm}_{\alpha\ell,\alpha\ell}$, $B^{(0)\pm}_{\alpha\ell,\alpha\ell}$ are matrices (at zeroth order proportional to the identity) determined by the value of the coefficients of $\left(\frac{1}{r-1}\right)^{\pm\nu}$ of the zeroth order near-horizon $\alpha\ell$-th solution with near horizon initial condition at the matching point. It is in principle straightforward to include the corrections of first order of ω in the coefficients, by using the next order expansion in the far region $r-1$. This yields $A^{(0)\pm}(\omega) = A^{(0)\pm}(0) + \omega \partial_\omega A^{(0)\pm}(0) + ...$ This matching procedure makes the dependence of these coefficients on ω quite clear.

Similar to the zeroth order solution, we can also obtain the coefficients $A^{(i)}_{\alpha\ell,\beta\ell'}$ and $B^{(i)}_{\alpha\ell,\beta\ell'}$ from matching the first and second order far region equations of motion with the near-horizon solutions. The difference is two-fold. (1) Due to the nonlinear behavior of the near-horizon solutions, the matrices are no-longer proportional to the identity. At first and higher order in ϵ the $\alpha\ell$-th infalling boundary condition can "source" a $\beta \neq \alpha, \ell \neq \ell'$-th far region solution. (2) The first or second order equations are inhomogenous, so we have to also be careful about matching the inhomogenous terms at the matching point. The far region equations, however, do not depend on ω and are still linear. If we are only interested in the ω-behavior, we can therefore still get expressions for the boundary coefficients of the first order or second order solutions that are as concise as the zeroth order one.

This constructs order by order in the modulation ϵ the matrices $A = A^{(0)} + \epsilon A^{(1)} + \dots$ and $B = B^{(0)} + \epsilon B^{(1)} + \dots$ whose ratio determines the boundary Green's function. To obtain the Green's function up to the second order, we can truncate the series for the diagonal elements of the matrices at second order $A_{\alpha\ell,\alpha\ell} = A^{(0)}_{\alpha\ell,\alpha\ell} + \epsilon^2 A^{(2)}_{\alpha\ell,\alpha\ell}$, $B_{\alpha\ell,\alpha\ell} = B^{(0)}_{\alpha\ell,\alpha\ell} + \epsilon^2 B^{(2)}_{\alpha\ell,\alpha\ell}$ (we use here the fact that first order contribution to the diagonal terms vanishes.) and off-diagonal terms to first order. The latter means that only terms with $\ell' = \ell \pm 1$ are nonvanishing and equal $A_{\alpha\ell,\alpha'\ell\pm1} = \epsilon A^{(1)}_{\alpha\ell,\alpha'\ell\pm1}$ or $B_{\alpha\ell,\alpha'\ell\pm1} = \epsilon B^{(1)}_{\alpha\ell,\alpha'\ell\pm1}$. After matching to the near region we can then write out the relevant elements of these

matrices as (here $\ell' = \ell \pm 1$)

$$
\begin{aligned}
A^{(0)}_{\alpha\ell,\alpha\ell} &= A^{(0)-}_{\alpha\ell,\alpha\ell} v^{(0,\ell)}_{-\alpha 2} + \tilde{\mathcal{G}}^{\ell}_{\alpha \mathrm{IR}} A^{(0)+}_{\alpha\ell,\alpha\ell} v^{(0,\ell)}_{+\alpha 2} \omega^{2\nu_{k_\ell}}, \\
B^{(0)}_{\alpha\ell,\alpha\ell} &= B^{(0)-}_{\alpha\ell,\alpha\ell} v^{(0,\ell)}_{-\alpha 1} + \tilde{\mathcal{G}}^{\ell}_{\alpha \mathrm{IR}} B^{(0)+}_{\alpha\ell,\alpha\ell} v^{(0,\ell)}_{+\alpha 1} \omega^{2\nu_{k_\ell}}, \\
A^{(1)}_{\alpha\ell,\beta\ell'} &= A^{(1,1)}_{\alpha\ell,\beta\ell'} \tilde{n_1}^{\ell}_{\alpha 2\beta\ell'} \omega^{\nu_{k_\ell}+\nu_{k_{\ell'}}} + A^{(1,3)}_{\alpha\ell,\beta\ell'} n_{3\alpha 2\beta\ell'}^{\ell} \omega^{2\nu_{k_{\ell'}}} + A^{(1,4)}_{\alpha\ell,\beta\ell'} n_{4\alpha 2\beta\ell'}^{\ell}, \\
B^{(1)}_{\alpha\ell,\beta\ell'} &= B^{(1,1)}_{\alpha\ell,\beta\ell'} \tilde{n_1}^{\ell}_{\alpha 1\beta\ell'} \omega^{\nu_{k_\ell}+\nu_{k_{\ell'}}} + B^{(1,3)}_{\alpha\ell,\beta\ell'} n_{3\alpha 1\beta\ell'}^{\ell} \omega^{2\nu_{k_{\ell'}}} + B^{(1,4)}_{\alpha\ell,\beta\ell'} n_{4\alpha 1\beta\ell'}^{\ell}, \\
A^{(2)}_{\alpha\ell,\alpha\ell} &= \big(A^{(2,1)}_{\alpha\ell} \tilde{s_1}^{\ell}_{\alpha 2} + A^{(2,4)}_{\alpha\ell} s_{4\alpha 2}^{\ell}\big)\omega^{2\nu_{k_\ell}} + \sum_{\ell'} A^{(2,3)}_{\alpha\ell,\ell'} s_{3\alpha 2\ell'}^{\ell} \omega^{\nu_{k_\ell}+\nu_{k_{\ell'}}} + \tilde{A}^{(2,4)}_{\alpha\ell} \tilde{s}_{4\alpha 2}^{\ell} \omega^{2\nu_{k_\ell}} \ln\omega + A^{(2,5)}_{\alpha\ell} s_{5\alpha 2}^{\ell}, \\
B^{(2)}_{\alpha\ell,\alpha\ell} &= \big(B^{(2,1)}_{\alpha\ell} \tilde{s_1}^{\ell}_{\alpha 1} + B^{(2,4)}_{\alpha\ell} s_{4\alpha 1}^{\ell}\big)\omega^{2\nu_{k_\ell}} + \sum_{\ell'} B^{(2,3)}_{\alpha\ell,\ell'} s_{3\alpha 1\ell'}^{\ell} \omega^{\nu_{k_\ell}+\nu_{k_{\ell'}}} + \tilde{B}^{(2,4)}_{\alpha\ell} \tilde{s}_{4\alpha 1}^{\ell} \omega^{2\nu_{k_\ell}} \ln\omega + B^{(2,5)}_{\alpha\ell} s_{5\alpha 1}^{\ell}
\end{aligned}
\tag{4.51}
$$

for the nondegenerate case. The parenthesized superscripts now refer to the different building blocks $n^{\ell}_{i\alpha j\beta\ell'}$ and $s^{\ell}_{i\alpha j\beta\ell'}$. For the degenerate case when $\nu_{k_\ell} = \nu_{k_{\ell'}}$ we find

$$
\begin{aligned}
A^{(0)}_{\alpha\ell,\alpha\ell} &= A^{(0)-}_{\alpha\ell,\alpha\ell} v^{(0,\ell)}_{-\alpha 2} + \tilde{\mathcal{G}}^{\ell}_{\alpha \mathrm{IR}} A^{(0)+}_{\alpha\ell,\alpha\ell} v^{(0,\ell)}_{+\alpha 2} \omega^{2\nu_{k_\ell}}, \\
B^{(0)}_{\alpha\ell,\alpha\ell} &= B^{(0)-}_{\alpha\ell,\alpha\ell} v^{(0,\ell)}_{-\alpha 1} + \tilde{\mathcal{G}}^{\ell}_{\alpha \mathrm{IR}} B^{(0)+}_{\alpha\ell,\alpha\ell} v^{(0,\ell)}_{+\alpha 1} \omega^{2\nu_{k_\ell}}, \\
A^{(1)}_{\alpha\ell,\beta\ell'} &= \big(A^{(1,1)}_{\alpha\ell,\beta\ell'} \tilde{d_1}^{\ell}_{\alpha 2\beta\ell'} \omega^{2\nu_{k_\ell}} + A^{(1,4)}_{\alpha\ell,\beta\ell'} d_{4\alpha 2\beta\ell'}^{\ell} \omega^{2\nu_{k_\ell}}\big) + A^{(1,2)}_{\alpha\ell,\beta\ell'} d_{3\alpha 2\beta\ell'}^{\ell} + 2A^{(1,2)}_{\alpha\ell,\beta\ell'} d_{3\alpha 2\beta\ell'}^{\ell} \omega^{2\nu_{k_\ell}} \ln\omega, \\
B^{(1)}_{\alpha\ell,\beta\ell'} &= \big(B^{(1,1)}_{\alpha\ell,\beta\ell'} \tilde{d_1}^{\ell}_{\alpha 1\beta\ell'} \omega^{2\nu_{k_\ell}} + B^{(1,4)}_{\alpha\ell,\beta\ell'} d_{4\alpha 1\beta\ell'}^{\ell} \omega^{2\nu_{k_\ell}}\big) + B^{(1,2)}_{\alpha\ell,\beta\ell'} d_{3\alpha 1\beta\ell'}^{\ell} + 2B^{(1,2)}_{\alpha\ell,\beta\ell'} d_{3\alpha 1\beta\ell'}^{\ell} \omega^{2\nu_{k_\ell}} \ln\omega, \\
A^{(2)}_{\alpha\ell,\alpha\ell} &= \big(A^{(2,1)}_{\alpha\ell} \tilde{\mathbf{s}_1}^{\ell}_{\alpha 2} + A^{(2,5)}_{\alpha\ell} \mathbf{s}_{5\alpha 2}^{\ell} + A^{(2,10)}_{\alpha\ell} \mathbf{s}_{10\alpha 2}^{\ell}\big)\omega^{2\nu_{k_\ell}} + \big(A^{(2,3)}_{\alpha\ell} \tilde{\mathbf{s}}_{3\alpha 2\ell'}^{\ell} + A^{(2,7)}_{\alpha\ell} \tilde{\mathbf{s}}_{7\alpha 2\ell'}^{\ell}\big)\omega^{2\nu_{k_\ell}} \ln\omega \\
&\quad + \big(A^{(2,6)}_{\alpha\ell} \mathbf{s}_{6\alpha 2}^{\ell} + A^{(2,11)}_{\alpha\ell} \mathbf{s}_{11\alpha 2}^{\ell}\big) + A^{(2,8)}_{\alpha\ell} \tilde{\mathbf{s}}_{8\alpha 2\ell'}^{\ell} \omega^{2\nu_{k_\ell}} (\ln\omega)^2 + (\text{terms from non-degenerate } \ell''), \\
B^{(2)}_{\alpha\ell,\alpha\ell} &= \big(B^{(2,1)}_{\alpha\ell} \tilde{\mathbf{s}}_{1\alpha 1}^{\ell} + B^{(2,5)}_{\alpha\ell} \mathbf{s}_{5\alpha 1}^{\ell} + B^{(2,10)}_{\alpha\ell} \mathbf{s}_{10\alpha 1}^{\ell}\big)\omega^{2\nu_{k_\ell}} + \big(B^{(2,3)}_{\alpha\ell} \tilde{\mathbf{s}}_{3\alpha 1\ell'}^{\ell} + B^{(2,7)}_{\alpha\ell} \tilde{\mathbf{s}}_{7\alpha 1\ell'}^{\ell}\big)\omega^{2\nu_{k_\ell}} \ln\omega \\
&\quad + \big(B^{(2,6)}_{\alpha\ell} \mathbf{s}_{6\alpha 1}^{\ell} + B^{(2,11)}_{\alpha\ell} \mathbf{s}_{11\alpha 1}^{\ell}\big) + B^{(2,8)}_{\alpha\ell} \tilde{\mathbf{s}}_{8\alpha 1\ell'}^{\ell} \omega^{2\nu_{k_\ell}} (\ln\omega)^2 + (\text{terms from non-degenerate } \ell'')
\end{aligned}
\tag{4.52}
$$

All the coefficients $A^{(n,j)}$, $B^{(n,j)}$ are real numbers, which depend on the momentum k, but are only the leading term in an analytic expansion in ω. Including the corrections due to sub-leading terms in order $1/(r-1)$ in the equations obtains the subleading powers of ω for each of these coefficients $A^{(n,j)} = \sum_{l=0}^{\infty} A^{(n,j,l)} \omega^l$ etc.

4.3 The full retarded Green's function

The final non-trivial step to obtain the full retarded Green's functions, is to invert the matrix A. For non-degenerate momenta $\nu_{k_\ell} \neq \nu_{k'_\ell}$, up to the second order in ϵ the determinant of A equals

$$
\begin{aligned}
\det A = \prod_{\alpha\ell} (A^{(0)}_{\alpha\ell,\alpha\ell} + \epsilon^2 A^{(2)}_{\alpha\ell,\alpha\ell}) \Big(1 - \epsilon^2 \big[\sum_{\ell'\alpha'} \frac{A^{(1)}_{\alpha'\ell',\alpha'\ell'+1} A^{(1)}_{\alpha'\ell'+1,\alpha'\ell'}}{A^{(0)}_{\alpha'\ell',\alpha'\ell'} A^{(0)}_{\alpha'\ell'+1,\alpha'\ell'+1}} \\
+ \sum_{\ell'} \frac{A^{(1)}_{1\ell',2\ell'+1} A^{(1)}_{2\ell'+1,1\ell'}}{A^{(0)}_{1\ell',1\ell'} A^{(0)}_{2\ell'+1,2\ell'+1}} + \sum_{\ell'} \frac{A^{(1)}_{2\ell',1\ell'+1} A^{(1)}_{1\ell'+1,2\ell'}}{A^{(0)}_{2\ell',2\ell'} A^{(0)}_{1\ell'+1,1\ell'+1}} \big] \Big)
\end{aligned}
\tag{4.53}
$$

and up to same order ϵ^2 the algebraic cofactors of A are

$$\begin{aligned}
\Delta_{\alpha\ell,\beta\ell\pm1} &= -\epsilon\frac{A^{(1)}_{\beta\ell\pm1,\alpha\ell}}{A^{(0)}_{\alpha\ell,\alpha\ell}A^{(0)}_{\beta\ell\pm1,\beta\ell\pm1}}\prod_{\alpha'\ell'}A^{(0)}_{\alpha'\ell',\alpha'\ell'};\\
\Delta_{\alpha\ell,\alpha\ell} &= \frac{\prod_{\alpha'\ell'}(A^{(0)}_{\alpha'\ell',\alpha'\ell'}+\epsilon^2A^{(2)}_{\alpha\ell,\alpha\ell})}{(A^{(0)}_{\alpha\ell,\alpha\ell}+\epsilon^2A^{(2)}_{\alpha\ell,\alpha\ell})}\Bigg(1-\epsilon^2\Big[\sum_{\ell'\alpha'}\frac{A^{(1)}_{\alpha'\ell',\alpha'\ell'+1}A^{(1)}_{\alpha'\ell'+1,\alpha'\ell'}}{A^{(0)}_{\alpha'\ell',\alpha'\ell'}A^{(0)}_{\alpha'\ell'+1,\alpha'\ell'+1}}+\sum_{\ell'}\frac{A^{(1)}_{1\ell',2\ell'+1}A^{(1)}_{2\ell'+1,1\ell'}}{A^{(0)}_{1\ell',1\ell'}A^{(0)}_{2\ell'+1,2\ell'+1}}\\
&\quad+\sum_{\ell'}\frac{A^{(1)}_{2\ell',1\ell'+1}A^{(1)}_{1\ell'+1,2\ell'}}{A^{(0)}_{2\ell',2\ell'}A^{(0)}_{1\ell'+1,1\ell'+1}}\Big]+\epsilon^2\sum_{\beta}\Big(\frac{A^{(1)}_{\beta\ell-1,\alpha\ell}A^{(1)}_{\alpha\ell,\beta\ell-1}}{A^{(0)}_{\beta\ell-1,\beta\ell-1}A^{(0)}_{\alpha\ell,\alpha\ell}}+\frac{A^{(1)}_{\beta\ell+1,\alpha\ell}A^{(1)}_{\alpha\ell,\beta\ell+1}}{A^{(0)}_{\beta\ell+1,\beta\ell+1}A^{(0)}_{\alpha\ell,\alpha\ell}}\Big)\Bigg);
\end{aligned}\tag{4.54}$$

where $\beta=\alpha,3-\alpha$. The full retarded Green's function is then

$$G_{\mathrm{R}\alpha\ell,\alpha\ell}=\frac{1}{\det A}\Bigg(\sum_{\beta=1,2}(B_{\alpha\ell,\beta\ell-1}\Delta_{\alpha\ell,\beta\ell-1}+B_{\alpha\ell,\beta\ell+1}\Delta_{\alpha\ell,\beta\ell+1})+B_{\alpha\ell,\alpha\ell}\Delta_{\alpha\ell,\alpha\ell}\Bigg).\tag{4.55}$$

In all expressions above, we have assumed that the diagonal elements in the A matrix are composed of both order 1 and order ϵ^2 parts and the off diagonal elements are of order ϵ so that the diagonal elements are always more important than the off diagonal ones. But we know that near the Fermi momentum of the zeroth order solution, the zeroth order part in the corresponding diagonal element becomes neglible — it vanishes at k_F — and the above expansion used to construct the Green's function does not hold. For the degenerate case, two of the diagonal elements are identical and both become subleading of order ϵ near the Fermi momentum. Degenerate eigenvalues is the familiar case from solid state textbooks and we will now show, that the intuition that a correct re-diagonalization will cause the opening of a band gap is correct. In the non-degenerate case, no band gap opens up — there is no eigenvalue mixing. However, correcting the violation of the naive expansion in ϵ will show that there are important second order corrections to the self-energy at the quasi-particle pole in the non-degenerate case.

5 Band structure and hybridized dissipation

We shall first discuss the physically most straightforward case: with degenerate eigenvalues any interaction will cause eigenvalue repulsion and the opening up of a band gap.

5.1 Band gap for the degenerate case

For the degenerate case, $\nu_{k_\ell}=\nu_{k'_\ell}$ with $\nu_{k_\ell}=\frac{1}{\sqrt{6}}\sqrt{k_\ell^2-q^2\frac{{\mu_0}^2}{6}}$ and $k_\ell=\sqrt{(k_x+\ell K)^2+k_y^2}$ the $k_y=0$ and $k_y\neq0$ cases are quite different. We first consider the special case $k_F=\frac{K}{2}$ (*i.e.* $k_x=\pm\frac{K}{2},k_y=0$). In this case, different spinor components do not interact (see eq. 3.15), so we can deal with the different spinor components independently. By definition the Fermi momentum is the value $k=k_F$ where the Green's function has a pole, i.e.

where the numerator $A_{\alpha\ell,\alpha\ell}(\omega = 0)$ vanishes at zero frequency, i.e. $A_{\alpha\ell,\alpha\ell}(k = k_F) \sim \omega a^{(0,1)}_{\alpha\ell,\alpha\ell} + \mathcal{O}(\omega^2, \epsilon^2)$. Recalling eq. (3.15) for this special case $k_y = 0$, we note that the equations for the two spinor components α decouple and are identical for each. Then it is straightforward to see that at zeroth order the momentum coefficient in the second Brillioun-zone ($\ell = 1$ with $k_x = -K/2$ or $\ell = -1$ with $k_x = K/2$) of the component α is equal to the momentum component of the other spin component $\beta = 3 - \alpha$ in the first Brillioun-zone ($\ell = 0$ and $k_x = -K/2$ or $k_x = K/2$ respectively). The degenerate term with $A_{\alpha\ell\alpha\ell}$ is therefore the *other* spinor component $\beta = 3 - \alpha$ in the neighboring Brillioun zone $\ell' = \ell - 1$ and hence $A_{\beta\ell-1;\beta\ell-1} = A_{\alpha\ell,\alpha\ell} \sim \mathcal{O}(\epsilon^2)$. Let us assume that it is both $A_{1\ell,1\ell}$ and $A_{2\ell-1,2\ell-1}$ which are of order $\omega a^{(1)} + \mathcal{O}(\epsilon^2)$ and much smaller than any other diagonal component of $A_{\alpha\ell,\beta\ell'}$. Substituting this in the expression for the retarded Green's function (4.55), we find

$$
\begin{aligned}
G_{\mathrm{R}1\ell,1\ell} &= \frac{B^{(0)}_{1\ell,1\ell} + \mathcal{O}(\epsilon^2)}{A^{(0)}_{1\ell,1\ell} + \epsilon^2 A^{(2)}_{1\ell,1\ell} - \epsilon^2\big(\frac{A^{(1)}_{1\ell,1\ell-1}A^{(1)}_{1\ell-1,1\ell}}{A^{(0)}_{1\ell-1,1\ell-1}} + \frac{A^{(1)}_{1\ell,1\ell+1}A^{(1)}_{1\ell+1,1\ell}}{A^{(0)}_{1\ell+1,1\ell+1}}\big) + \mathcal{O}(\epsilon^4)}, \\
G_{\mathrm{R}2\ell,2\ell} &= \frac{1 - \epsilon^2 \frac{A^{(1)}_{2\ell-1,2\ell-2}A^{(1)}_{2\ell-2,2\ell-1}}{A^{(0)}_{2\ell-2,2\ell-2}A^{(0)}_{2\ell-1,2\ell-1}}}{1 - \epsilon^2\big(\frac{A^{(1)}_{2\ell-1,2\ell}A^{(1)}_{2\ell,2\ell-1}}{A^{(0)}_{2\ell,2\ell}A^{(0)}_{2\ell-1,2\ell-1}} + \frac{A^{(1)}_{2\ell-1,2\ell-2}A^{(1)}_{2\ell-2,2\ell-1}}{A^{(0)}_{2\ell-2,2\ell-2}A^{(0)}_{2\ell-1,2\ell-1}}\big)} \left[\frac{B^{(0)}_{2\ell,2\ell}}{A^{(0)}_{2\ell,2\ell}} + \mathcal{O}(\epsilon^2)\right].
\end{aligned}
\tag{5.1}
$$

From the above formulae we see that near k_F, $G_{\mathrm{R}2\ell,2\ell}$ is regular while

$$
G_{\mathrm{R}1\ell,1\ell} \simeq \frac{B^{(0)}_{1\ell,1\ell}}{\omega - v_F(k_\ell - k_F) + \Sigma(\omega)}, \tag{5.2}
$$

where $\Sigma(\omega)$ denotes the self-energy. So there is no gap in this case. This may seem surprising. It is however a direct consequence of the fact that the holographic fermion spectral function has a chiral decomposition for $k_y = 0$. In the basis of Gamma-matrices (3.12) spin up particles ($\alpha = 1$) only have right-moving dispersion $\omega = k_x$, whereas spin down ($\alpha = 2$) particles only have left moving dispersion $\omega = -k_x$.[10] As noted in [38], in order to have a gap this chiral structure must be broken and interactions must be present that mix the two.

In the absence of a lattice any nonzero k_y solution can be again rotated to a chiral basis. In the presence of a lattice this rotation freedom is broken and these interactions occur for any $k_y \neq 0$ as we can directly see in (4.2). Now the degeneracy $\nu_{k_\ell} = \nu_{k_{\ell'}}$ leads to $A_{\alpha\ell,\alpha\ell} = A_{\alpha\ell-1,\alpha\ell-1}$. (For any $k_y \neq 0$, k_ℓ is always positive and (4.2), than immediately shows that now the same spinor component is degenerate between the first $\ell = 0$ and second $\ell = \pm 1$ Brillioun zones). As a result, near a zeroth order Fermi surface, both $A^{(0)}_{\alpha\ell,\alpha\ell}$ and $A^{(0)}_{\alpha\ell-1,\alpha\ell-1}$ become very small and comparable to the modulation order ϵ, and assuming

[10] The spin structure for holographic fermions has been studied in [39, 40].

that all other diagonal components of $A_{\alpha\ell,\beta\ell'}$ are much larger, the retarded Green's function equals

$$G_{\mathrm{R}\alpha\ell,\alpha\ell} = \frac{A^{(0)}_{\alpha\ell,\alpha\ell}B^{(0)}_{\alpha\ell,\alpha\ell} + \mathcal{O}(\epsilon^2)}{(A^{(0)}_{\alpha\ell,\alpha\ell} + \epsilon^2 A^{(2)}_{\alpha\ell,\alpha\ell})^2 - \epsilon^2 A^{(1)}_{\alpha\ell,\alpha\ell-1}A^{(1)}_{\alpha\ell-1,\alpha\ell} + \mathcal{O}(\epsilon^3)}. \tag{5.3}$$

Near $k_\ell = k_F, \omega = 0$, we have $A^{(0)}_{\alpha\ell,\alpha\ell} + \epsilon^2 A^{(2)}_{\alpha\ell,\alpha\ell} = \omega - v_F(k_\ell - k_F) + i(c_1 - ic_2)\omega^{2\nu_{k_\ell}}$ with v_F, c_1, c_2 are real and dependent on UV data. Assuming $2\nu_{k_\ell} > 1$, i.e. the original theory possessed a regular quasiparticle with linear dispersion liquid, we can ignore c_2 and find that Umklapp for degenerate momenta modifies the Green's function to

$$G_{\mathrm{R}\alpha\ell,\alpha\ell} \simeq \frac{(\omega - v_F(k_\ell - k_F))B_{\alpha\ell,\alpha\ell}}{(\omega - v_F(k_\ell - k_F))^2 - \Delta^2 + ic_1(\omega - v_F(k_\ell - k_F))\omega^{2\nu_{k_\ell}}} \tag{5.4}$$

where

$$\Delta^2 = \epsilon^2 A^{(1)}_{\alpha\ell,\alpha\ell-1}A^{(1)}_{\alpha\ell-1,\alpha\ell} = \epsilon^2\big(1 - \frac{1}{\sqrt{1+(2ak_y)^2}}\big)\mathfrak{a}^2_{k_\ell} \tag{5.5}$$

with $\mathfrak{a}_{k_\ell}$ a function of k_ℓ. The denominator shows a classic band gap[11] with two peaks at $\omega = v_F(k_\ell - k_F) \pm \Delta$. Note that the bandgap already appears at first order in ϵ, the second order corrections will only make a small quantitative change. The width of gap is therefore proportional to ϵ. The pole has shifted to $\omega \sim \Delta \sim \epsilon$ and its width is therefore of order $\epsilon^{2\nu_{k_\ell}}$. Recall that here $2\nu_{k_\ell} > 1$, so the width of the peaks is negligible comparing to the width of the gap. Thus the peaks are sharp.

Assuming the original quasiparticle was non-Fermi liquid-like, i.e. $2\nu_{k_\ell} < 1$, and near $k_\ell = k_F, \omega = 0$, $A_{\alpha\ell,\alpha\ell} = c_2\omega^{2\nu_{k_\ell}} - v_F(k_\ell - k_F) + ic_1\omega^{2\nu_{k_\ell}}$ we find the Umklapp modified Green's function

$$G_{\mathrm{R}\alpha\ell,\alpha\ell} \simeq \frac{(\omega^{2\nu_{k_\ell}} - v_F(k_\ell - k_F))B_{\alpha\ell,\alpha\ell}}{(\omega^{2\nu_{k_\ell}} - v_F(k_\ell - k_F))^2 - \Delta^2 + ic_1(\omega^{2\nu_{k_\ell}} - v_F(k_\ell - k_F))\omega^{2\nu_{k_\ell}}}. \tag{5.6}$$

This is a gapped system for non-linear dispersion with two peaks at $\omega^{2\nu_{k_\ell}} = v_F(k_\ell - k_F) \pm \Delta$. The instability of the original non-Fermi liquid quasiparticle now reflects itself in that the width of peak and the gap are of the same order $\epsilon^{1/2\nu_{k_\ell}}$. For the marginal case $2\nu_{k_\ell} = 1$, where near $k_\ell = k_F, \omega = 0$ we have $A_{\alpha\ell,\alpha\ell} = \omega + c_2\omega\ln\omega - v_F(k_\ell - k_F) + ic_1\omega\ln\omega$ one similarly concludes the presence of a bandgap.

We emphasize that the mechanism which leads to a gap is identical to the standard band structure in condensed matter theories: the occurence of degenerate eigenvalues which repel each other upon the inclusion of interactions between the different levels. In that sense the mechanism is similar to the holographic BCS gap in [38, 41] and [42, 43]. In essence, the fact that the holographic spectral function can be reproduced from a Dyson resummation

[11] To be explicit, all points on these two bands with finite ω are not strict poles because the imaginary part of the self-energy doesn't vanish but it is small. The existence of bands only depends on the real part of the denominator and the self energy can be ignored as long as it stays small throughout.

of a free fermion coupled to the local quantum critical AdS_2, a.k.a. semi-holography [13], guarantees that all these situations should simply recover the textbook gap. As we will see in the next subsection, however, the dissipative properties also change due to the lattice. And, correlated to this, we can then also show that the Green's function in the latticized AdS_2 metal do not possess a gap.

5.2 Hybridized dissipation around the gap and the AdS_2-metal Greens function on the lattice

The band gap in the presence of a Fermi surface is a first order in ϵ effect. Our analysis of the perturbative form of the retarded Green's function in section 4 already showed that the change in the dispersive properties occurs at second order in the modulation ϵ. In the case of a Fermi surface the dispersive properties show up as a modification of the self-energy, whereas for the AdS_2 metal they directly affect the defining characteristics of the spectral function. We shall discuss the case of a Fermi-surface (with a band gap) first.

5.2.1 Near the Fermi surface

Near the pole, the leading component $A^{(0)}_{\alpha\ell,\alpha\ell}$ becomes of the same order as the formally subleading $\mathcal{O}(\epsilon^2)$ corrections, so we should be very careful with small terms in the bracket in the formula (4.53) of $\det A$. We define

$$C=\sum_{\beta=1,2}\left(\frac{A^{(1)}_{\beta\ell-1,\alpha\ell}A^{(1)}_{\alpha\ell,\beta\ell-1}}{A_{\beta\ell-1,\beta\ell-1}A_{\alpha\ell,\alpha\ell}}+\frac{A^{(1)}_{\beta\ell+1,\alpha\ell}A^{(1)}_{\alpha\ell,\beta\ell+1}}{A_{\beta\ell+1,\beta\ell+1}A_{\alpha\ell,\alpha\ell}}\right). \tag{5.7}$$

Then for both the non-degenerate case as well as the degenerate case with $k_y=0$ the retarded Green's function becomes

$$\begin{aligned}G_{\mathrm{R}\alpha\ell,\alpha\ell}&\simeq\frac{1}{(A^{(0)}_{\alpha\ell,\alpha\ell}+\epsilon^2A^{(2)}_{\alpha\ell,\alpha\ell})(1-\epsilon^2C)}\left[B_{\alpha\ell,\alpha\ell}-\epsilon^2\sum_{\alpha'=1,2}\left(\frac{A^{(1)}_{\alpha'\ell-1,\alpha\ell}B^{(1)}_{\alpha\ell,\alpha'\ell-1}}{A^{(0)}_{\alpha'\ell-1,\alpha'\ell-1}}+\frac{A^{(1)}_{\alpha'\ell+1,\alpha\ell}B^{(1)}_{\alpha\ell,\alpha'\ell+1}}{A^{(0)}_{\alpha'\ell+1,\alpha'\ell+1}}\right)\right]\\&=\frac{B^{(0)}_{\alpha\ell,\alpha\ell}+\mathcal{O}(\epsilon^2)}{A^{(0)}_{\alpha\ell,\alpha\ell}+\epsilon^2(A^{(2)}_{\alpha\ell,\alpha\ell}-A^{(0)}_{\alpha\ell,\alpha\ell}C)+\mathcal{O}(\epsilon^4)}.\end{aligned} \tag{5.8}$$

A consistency check for the expression (5.8) is that it does not depend on the freedom to add arbitrary infalling homogenous solution at first or second order which we used to cancel the possible divergence related to $\omega\to 0$. The operation of adding them is equal to the transformation $A\to AU$ and $B\to BU$ with U a matrix of two-component spinors of which the non-zero elements are: $U_{1\alpha'\ell',\alpha'\ell'}=1,(\forall\alpha',\ell'),U_{1\beta\ell+1,\alpha\ell}=\epsilon\zeta^{(1)}$ or $U_{1\beta\ell-1,\alpha\ell}=\epsilon\zeta^{(1)}$ and $U_{2\alpha'\ell',\alpha'\ell'}=1,(\forall\alpha',\ell'\neq\alpha\ell),U_{2\alpha\ell,\alpha\ell}=1+\epsilon^2\zeta^{(2)}$ with $\zeta^{(i)}$ a constant. It is easy to show that formula (5.8) is invariant under these two operations up to order ϵ^2.

Here we are focussing on the diagonal elements of the Green's function. The off-diagonal elements of the Green's function will also contribute to the spectral weight in the

coordinate space. However, following the characteristics of the building blocks $A_{\alpha\ell,\beta\ell'}$ and $B_{\alpha\ell,\beta\ell'}$ the leading order contribution of the off-diagonal Green's function elements is of order ϵ. We will not study them explicitly in this paper and focus here only on the diagonal part.

For the non-degenerate case, we have (ungapped) quasi-particle poles when the denominator in (5.8) vanishes. Substituting the expression for C, this happens whenever

$$A^{(0)}_{\alpha\ell,\alpha\ell} + \epsilon^2 A^{(2)}_{\alpha\ell,\alpha\ell} - \epsilon^2 \sum_{\beta=1,2} \left(\frac{A^{(1)}_{\beta\ell-1,\alpha\ell} A^{(1)}_{\alpha\ell,\beta\ell-1}}{A^{(0)}_{\beta\ell-1,\beta\ell-1}} + \frac{A^{(1)}_{\beta\ell+1,\alpha\ell} A^{(1)}_{\alpha\ell,\beta\ell+1}}{A^{(0)}_{\beta\ell+1,\beta\ell+1}} \right) = 0. \tag{5.9}$$

The essence is now to extract the ω-dependence from this expression using the perturbative answers (4.51) we obtained for $A_{\alpha\ell,\alpha\ell}$, etc. Denoting the diagonal component of the retarded Green's function in its standard form

$$G_{\alpha\ell,\alpha\ell} = \frac{Z}{\omega - v_F(k - k_F) + \Sigma} + \dots \tag{5.10}$$

one finds after some laborious algebra that the self-energy

$$\begin{aligned} \Sigma = {} & \alpha_{\vec{k}} \omega^{2\nu_{\vec{k}}} + \beta^{(1)}_{\vec{k}} \omega^{2\nu_{\vec{k}-\vec{K}}} + \beta^{(2)}_{\vec{k}} \omega^{\nu_{\vec{k}}+\nu_{\vec{k}-\vec{K}}} + \beta^{(3)}_{\vec{k}} \omega^{2\nu_{\vec{k}}} \ln \omega \\ & + \beta^{(4)}_{\vec{k}} \omega^{\nu_{\vec{k}}+\nu_{\vec{k}+\vec{K}}} + \beta^{(5)}_{\vec{k}} \omega^{2\nu_{\vec{k}+\vec{K}}} + \dots \end{aligned} \tag{5.11}$$

where $\alpha_{\vec{k}} \sim \mathcal{O}(1)$ and $\beta^{(i)}_{\vec{k}} \sim \mathcal{O}(\epsilon^2)$ with $i = 1, ...5$. These coefficients are complex functions of k. The concrete formula of the parameters can be found in the appendix (A.8-A.15).

This is our main result whose physics we discussed in the beginning. For this, note that the Brillioun zone mixing terms $\omega^{\nu_{\vec{k}}+\nu_{\vec{k}\pm\vec{K}}}$ are never the leading terms in the IR. For the purpose of the IR physics, we may therefore truncate the self-energy to

$$\Sigma = \alpha_{\vec{k}} \omega^{2\nu_{\vec{k}}} + \beta^{(1)}_{\vec{k}} \omega^{2\nu_{\vec{k}-\vec{K}}} + \beta^{(3)}_{\vec{k}} \omega^{2\nu_{\vec{k}}} \ln \omega + \beta^{(5)}_{\vec{k}} \omega^{2\nu_{\vec{k}+\vec{K}}} + \dots \tag{5.12}$$

This is eq. (2.5).

Performing the same steps for the degenerate case with $k_y = 0$, one finds the diagonal Green's function (see eq. (5.2))

$$G_{\alpha\ell,\alpha\ell} = \frac{Z}{\omega - v_F(k - k_F) + \Sigma} + \dots \tag{5.13}$$

with

$$\begin{aligned} \Sigma = {} & \alpha_{\vec{k}} \omega^{2\nu_{\vec{k}}} + \beta^{(1)}_{\vec{k}} \omega^{2\nu_{\vec{k}-\vec{K}}} + \beta^{(2)}_{\vec{k}} \omega^{\nu_{\vec{k}}+\nu_{\vec{k}-\vec{K}}} + \beta^{(3)}_{\vec{k}} \omega^{2\nu_{\vec{k}}} \ln \omega + \tilde{\beta}_{\vec{k}} \omega^{2\nu_{\vec{k}}} (\ln \omega)^2 \\ & + \beta^{(4)}_{\vec{k}} \omega^{\nu_{\vec{k}}+\nu_{\vec{k}+\vec{K}}} + \beta^{(5)}_{\vec{k}} \omega^{2\nu_{\vec{k}+\vec{K}}} + \dots \end{aligned} \tag{5.14}$$

where $\alpha_{\vec{k}} \sim \mathcal{O}(1)$ and $\tilde{\beta}$, $\beta^{(i)}_{\vec{k}} \sim \mathcal{O}(\epsilon^2)$ with $i = 1, ...5$. The concrete formula of the parameters can be obtained similarly as the non-degenerate case. The distinction with the

non-degenerate case is that the logarithmic term correction to the naive dispersion is now of the form $(\ln\omega)^2$. Here we only list the result for $\tilde{\beta}_{\vec{k}}$

$$\tilde{\beta}_{\vec{k}} \sim \frac{A^{(2,8)}_{\alpha\ell}\tilde{\mathbf{s}}^{\ell}_{8\alpha 2\ell'}}{A^{(0+)}_{\alpha\ell,\alpha\ell}v^{(0,\ell)}_{+\alpha 2}\tilde{\mathcal{G}}^{\ell}_{\alpha}}. \tag{5.15}$$

For the degenerate case with $k_y \neq 0$ where the poles repel to form a gap, the dispersion part changes due to the formation of the gap, see (5.4) and (5.6). In this case, the self energy will also get corrections with the formulae (5.14).

We emphasize here that the form of the self-energy means that it cannot be simply interpreted as some local quantum critical (i.e. pure AdS_2) Green's function. The solution is no longer a pure power of ω, but a polynomial. At the same time the near-far matching construction does reflect that the self-energy is governed by the IR-dynamics. This, however, is a latticized version of the near-horizon AdS_2 region to which we now turn.

5.2.2 AdS_2 metal

In the AdS_2 metal regime of parameters the full spectral function is related to the IR-spectral function. In essence this is due to the fact that there is no pole in the spectral function, i.e. $A_{\alpha\ell,\alpha\ell} \neq 0$ always. This allows us to immediately extract the spectral function in a perturbation expansion in ϵ. The Green's function itself equals

$$G_{\mathrm{R}\alpha\ell,\alpha\ell} = \frac{B^{(0)}_{\alpha\ell,\alpha\ell}}{A^{(0)}_{\alpha\ell,\alpha\ell}} + \epsilon^2\left(\frac{B^{(0)}_{\alpha\ell,\alpha\ell}}{A^{(0)}_{\alpha\ell,\alpha\ell}}C - \sum_{\beta}\frac{B^{(1)}_{\alpha\ell,\beta\ell\pm1}A^{(1)}_{\beta\ell\pm1,\alpha\ell}}{A^{(0)}_{\alpha\ell,\alpha\ell}A^{(1)}_{\beta\ell\pm1,\beta\ell\pm1}}\right) + \mathcal{O}(\epsilon^4) \tag{5.16}$$

where C is defined as in (5.7), and the spectral function at low ω is thus

$$\mathrm{Im}G_{\mathrm{R}\alpha\ell,\alpha\ell} \simeq \mathrm{Im}\Sigma \tag{5.17}$$

with Σ the same formula of the self-energy as above in (5.11) and (5.14) with different values of coefficients. As in [4], this directly follows from the fact that the analytic terms in ω in $A^{(0)}_{\alpha\ell,\alpha\ell}$ are real (for real ν_k) and that all non-analytic terms in $B^{(0)}_{\alpha\ell,\alpha\ell}$ are of higher order in ω.

6 Technical Conclusions

Eqns. (5.4), (5.11), (5.14) and (5.17) are our main conclusions of lattice effects on holographic single fermion spectral functions. Here the lattice is encoded by a periodic correction to the gauge potential in RN AdS black hole background dual to a strongly coupled $2+1$ dimensional field theory at finite density. We have already discussed the main physics of these results in the beginning, section 2. In the quasi-Fermi-surface regime ($q \gg m$) one finds a gap and the mechanism for the presence of the gap is similar to the standard condensed matter physics: the degeneracy from the interaction between different levels

gives the gap. The gap disappears when such kinds of interaction turned off. The more interesting physics is that related to the AdS_2 sector. In the quasi-Fermi surface regime this is responsible for the dispersive properties of the Fermi-surface excitations. In the opposite ($q \ll m$) AdS_2 metal regime it itself controls the IR physics. The effect of the lattice is to allow Umklapp contributions $\omega^{2\nu_{\vec{k}\pm\vec{K}}}$ to the characteristic local quantum critical scaling $\omega^{2\nu_{\vec{k}}}$. These essentially shift more spectral weight to lower energies.

At the technical level we made a number of assumptions to obtain our results. For convenience we have chosen the dual spacetime geometry as RN black hole with only A_t modified to encode the lattice effect, i.e. we neglected the backreaction of the lattice effect to the metric field. One immediate question is what would happen when the first order gravity corrections appears. We have argued in section 3 that the understanding of level repulsion and lattice symmetries should not change the qualitative features of our result. Nevertheless it would be good to confirm this. Such kinds of geometry where the lattice effect to the metric field was also studied has been recently considered in [26] (see also [21, 44–46]). It would be very interesting to study the spectral functions of the probe fermion in these backgrounds.

In addition there are several ways to generalize our methods.

- The most obvious next step is the compute the spatially local Green's function $G(\omega; x, x)$ relevant for scanning tunneling spectroscopy rather then ARPES. In momentum space this implies that we shall also need to evaluate the $G(\omega, k, k + K)$ Green's function.

- One can consider a more general potential, such as the gauge potentials with higher order Fourier components $\mu_1(x + 2\pi a) = \mu_1(x) = \sum_n \epsilon_n \cos \frac{nx}{a}$ or other lattice structure, e.g. the canonical two-dimensional square or rectangular lattice $\mu_1(x + 2\pi a, y + 2\pi b) = \mu_1(x, y)$.

- In the approach here we worked perturbatively in the weak potential limit. In condensed matter physics, another interesting approach to the band structure is the tight binding model. Holographically these are presumably closer related to brane-models of the type considered in [30, 47]. Perhaps there might be a way to interpolate between them.

We hope to return to these issues in the future.

Acknowledgments

We thank A. Beekman, B. van Rees, A. Parnachev, S. Sachdev, J-H She, A. O. Starinets, K. Wu for useful discussions. This research is supported in part by a Spinoza Award (J. Zaanen) from the Netherlands Organisation for Scientific Research (NWO) and by the Dutch Foundation for Fundamental Research on Matter (FOM).

A Coefficients

In this appendix, we collect the coefficients appeared in eqns. (4.28, 4.37, 4.41, 4.44, 5.11). These coefficients do not depend on ω and ε and are finite.

- The coefficients in (4.28)

$$
\begin{aligned}
n_{1\alpha j\beta\ell'}^{\ell} &= \omega^{-\nu_{k_{\ell'}}}\int_{\infty}^{\varepsilon} dz\frac{\eta_{1\alpha j}^{\ell}X_{(\alpha j,\beta\ell')}^{\ell}}{c_{\alpha j}^{\ell}h_{\alpha j}z^2} - \frac{qM_{\alpha\beta,\ell\ell'}}{12\nu_{k_\ell}}\bigg(\frac{q\mu_0}{3}+(-1)^{\alpha+j+1}\frac{k_\ell}{\sqrt{6}}\\
&\quad -(-1)^{\beta+j+1}\frac{k_{\ell'}}{\sqrt{6}}\bigg)\bigg[\frac{\varepsilon^{-\nu_{k_\ell}-\nu_{k_{\ell'}}}}{-\nu_{k_\ell}-\nu_{k_{\ell'}}}v_{-\beta j}^{(0,\ell')}+\frac{\varepsilon^{-\nu_{k_\ell}+\nu_{k_{\ell'}}}}{-\nu_{k_\ell}+\nu_{k_{\ell'}}}\tilde{\mathcal{G}}_{\beta}^{\ell'}v_{+\beta j}^{(0,\ell')}\bigg];\\
n_{2\alpha j\beta\ell'}^{\ell} &= -\omega^{-\nu_{k_{\ell'}}}\int_{\infty}^{\varepsilon} dz\frac{\eta_{2\alpha j}^{\ell}X_{(\alpha j,\beta\ell')}^{\ell}}{c_{\alpha j}^{\ell}h_{\alpha j}z^2} + \frac{qM_{\alpha\beta,\ell\ell'}}{12\nu_{k_\ell}}\bigg(\frac{q\mu_0}{3}+(-1)^{\alpha+j+1}\frac{k_\ell}{\sqrt{6}}\\
&\quad -(-1)^{\beta+j+1}\frac{k_{\ell'}}{\sqrt{6}}\bigg)\bigg[\frac{\varepsilon^{\nu_{k_\ell}-\nu_{k_{\ell'}}}}{\nu_{k_\ell}-\nu_{k_{\ell'}}}v_{-\beta j}^{(0,\ell')}+\frac{\varepsilon^{\nu_{k_\ell}+\nu_{k_{\ell'}}}}{\nu_{k_\ell}+\nu_{k_{\ell'}}}\tilde{\mathcal{G}}_{\beta}^{\ell'}v_{+\beta j}^{(0,\ell')}\bigg];\\
n_{3\alpha j\beta\ell'}^{\ell} &= -\frac{qM_{\alpha\beta,\ell\ell'}}{6(\nu_{k_\ell}^2-\nu_{k_{\ell'}}^2)}\bigg(\frac{q\mu_0}{3}+(-1)^{\alpha+j+1}\frac{k_\ell}{\sqrt{6}}-(-1)^{\beta+j+1}\frac{k_{\ell'}}{\sqrt{6}}\bigg)\tilde{\mathcal{G}}_{\beta}^{\ell'}v_{+\beta j}^{(0,\ell')};\\
n_{4\alpha j\beta\ell'}^{\ell} &= -\frac{qM_{\alpha\beta,\ell\ell'}}{6(\nu_{k_\ell}^2-\nu_{k_{\ell'}}^2)}\bigg(\frac{q\mu_0}{3}+(-1)^{\alpha+j+1}\frac{k_\ell}{\sqrt{6}}-(-1)^{\beta+j+1}\frac{k_{\ell'}}{\sqrt{6}}\bigg)v_{-\beta j}^{(0,\ell')}
\end{aligned}
\tag{A.1}
$$

  where

$$
c_{\alpha j}^{\ell} = \frac{2\nu_{k_\ell}}{\frac{q\mu_0}{6}+(-1)^{\alpha+j+1}\frac{k_\ell}{\sqrt{6}}}. \tag{A.2}
$$

- The coefficients in (4.37)

$$
\begin{aligned}
s_{1\alpha j}^{\ell} &= \omega^{-\nu_{k_\ell}}\int_{\infty}^{\varepsilon} dz\frac{\tilde{\eta}_{1\alpha j}^{\ell}Y_{\alpha j}^{\ell}}{c_{\alpha j}^{\ell}z^2h_{\alpha j}} + \frac{q}{6c_{\alpha j}^{\ell}}\sum_{\beta;\ell'=\ell\pm1}M_{\alpha\beta,\ell\ell'}\bigg[\frac{\varepsilon^{\nu_{k_{\ell'}}-\nu_{k_\ell}}}{\nu_{k_{\ell'}}-\nu_{k_\ell}}N_{1\beta j,\alpha\ell}^{\ell'}\\
&\quad + N_{3\beta j,\alpha\ell}^{\ell'}(\ln\varepsilon+\frac{1}{2\nu_{k_\ell}}) - \frac{\varepsilon^{-2\nu_{k_\ell}}}{2\nu_{k_\ell}}N_{4\beta j,\alpha\ell}^{\ell'}\bigg];\\
s_{2\alpha j}^{\ell} &= -\omega^{-\nu_{k_\ell}}\int_{\infty}^{\varepsilon} dz\frac{\tilde{\eta}_{2\alpha j}^{\ell}Y_{\alpha j}^{\ell}}{c_{\alpha j}^{\ell}z^2h_{\alpha j}} - \frac{q}{6c_{\alpha j}^{\ell}}\sum_{\beta,\ell'=\ell\pm1}M_{\alpha\beta,\ell\ell'}\bigg[\frac{\varepsilon^{\nu_{k_{\ell'}}+\nu_{k_\ell}}}{\nu_{k_{\ell'}}+\nu_{k_\ell}}N_{1\beta j,\alpha\ell}^{\ell'}\\
&\quad + N_{3\beta j,\alpha\ell}^{\ell'}\frac{\varepsilon^{2\nu_{k_\ell}}}{2\nu_{k_\ell}} + N_{4\beta j,\alpha\ell}^{\ell'}\big(\ln\varepsilon-\frac{1}{2\nu_{k_\ell}}\big)\bigg];\\
s_{3\alpha j\ell'}^{\ell} &= \frac{q}{6c_{\alpha j}^{\ell}}\sum_{\beta}M_{\alpha\beta,\ell\ell'}\frac{2\nu_{k_\ell}}{\nu_{k_\ell}^2-\nu_{k_{\ell'}}^2}N_{1\beta j,\alpha\ell}^{\ell'};\\
s_{4\alpha j}^{\ell} &= -\frac{q}{6c_{\alpha j}^{\ell}}\sum_{\beta,\ell'=\ell\pm1}M_{\alpha\beta,\ell\ell'}N_{3\beta j,\alpha\ell}^{\ell'};\\
s_{5\alpha j}^{\ell} &= \frac{q}{6c_{\alpha j}^{\ell}}\sum_{\beta,\ell'=\ell\pm1}M_{\alpha\beta,\ell\ell'}N_{4\beta j,\alpha\ell}^{\ell'}
\end{aligned}
\tag{A.3}
$$

with

$$
\begin{aligned}
N_{1\beta j,\alpha\ell}^{\ell'} &= \tilde{n_1}_{\beta j,\alpha\ell}^{\ell'} - \frac{(-1)^j \nu_{k_{\ell'}}}{\frac{q\mu_0}{6} + (-1)^{\alpha+j+1}\frac{k_\ell}{\sqrt{6}}} \tilde{n_1}_{\beta l,\alpha\ell}^{\ell'};\\
N_{3\beta j,\alpha\ell}^{\ell'} &= n_{3\beta j,\alpha\ell}^{\ell'} - \frac{(-1)^j \nu_{k_\ell}}{\frac{q\mu_0}{6} + (-1)^{\alpha+j+1}\frac{k_\ell}{\sqrt{6}}} n_{3\beta l,\alpha\ell}^{\ell'};\\
N_{4\beta j,\alpha\ell}^{\ell'} &= n_{4\beta j,\alpha\ell}^{\ell'} + \frac{(-1)^j \nu_{k_\ell}}{\frac{q\mu_0}{6} + (-1)^{\alpha+j+1}\frac{k_\ell}{\sqrt{6}}} n_{4\beta l,\alpha\ell}^{\ell'}.
\end{aligned}
\tag{A.4}
$$

- The coefficients in (4.41)

$$
\begin{aligned}
d_{1\alpha j\beta\ell'}^{\ell} &= \omega^{-\nu_{k_{\ell'}}} \int_\infty^\varepsilon dz \frac{\eta_{1\alpha j}^{\ell} X_{(\alpha j,\beta\ell')}^{\ell}}{c_{\alpha j}^{\ell} h_{\alpha j} z^2} - \frac{q M_{\alpha\beta,\ell\ell'}}{12\nu_{k_\ell}} \Big(\frac{q\mu_0}{3} + (-1)^{\alpha+j+1}\frac{k_\ell}{\sqrt{6}}\\
&\quad - (-1)^{\beta+j+1}\frac{k_{\ell'}}{\sqrt{6}} \Big) \Big[\frac{\varepsilon^{-2\nu_{k_\ell}}}{-2\nu_{k_\ell}} v_{-\beta j}^{(0,\ell')} + \tilde{\mathcal{G}}_\beta^{\ell'} v_{+\beta j}^{(0,\ell')} \ln\varepsilon \Big]\\
&\quad - \frac{q M_{\alpha\beta,\ell\ell'}}{24\nu_{k_\ell}^2} \Big(\frac{q\mu_0}{3} + (-1)^{\alpha+j+1}\frac{k_\ell}{\sqrt{6}} - (-1)^{\beta+j+1}\frac{k_{\ell'}}{\sqrt{6}} \Big) \tilde{\mathcal{G}}_\beta^{\ell'} v_{+\beta j}^{(0,\ell')};\\
d_{2\alpha j\beta\ell'}^{\ell} &= -\omega^{-\nu_{k_{\ell'}}} \int_\infty^\varepsilon dz \frac{\eta_{2\alpha j}^{\ell} X_{(\alpha j,\beta\ell')}^{\ell}}{c_{\alpha j}^{\ell} h_{\alpha j} z^2} + \frac{q M_{\alpha\beta,\ell\ell'}}{12\nu_{k_\ell}} \Big(\frac{q\mu_0}{3} + (-1)^{\alpha+j+1}\frac{k_\ell}{\sqrt{6}}\\
&\quad - (-1)^{\beta+j+1}\frac{k_{\ell'}}{\sqrt{6}} \Big) \Big[v_{-\beta j}^{(0,\ell')} \ln\varepsilon + \frac{\varepsilon^{\nu_{k_\ell}+\nu_{k_{\ell'}}}}{\nu_{k_\ell}+\nu_{k_{\ell'}}} \tilde{\mathcal{G}}_\beta^{\ell'} v_{+\beta j}^{(0,\ell')} \Big]\\
&\quad - \frac{q M_{\alpha\beta,\ell\ell'}}{24\nu_{k_\ell}^2} \Big(\frac{q\mu_0}{3} + (-1)^{\alpha+j+1}\frac{k_\ell}{\sqrt{6}} - (-1)^{\beta+j+1}\frac{k_{\ell'}}{\sqrt{6}} \Big) v_{-\beta j}^{(0,\ell')};\\
d_{3\alpha j\beta\ell'}^{\ell} &= \frac{q M_{\alpha\beta,\ell\ell'}}{12\nu_{k_\ell}} \Big(\frac{q\mu_0}{3} + (-1)^{\alpha+j+1}\frac{k_\ell}{\sqrt{6}} - (-1)^{\beta+j+1}\frac{k_{\ell'}}{\sqrt{6}} \Big) \tilde{\mathcal{G}}_\beta^{\ell'} v_{+\beta j}^{(0,\ell')};\\
d_{4\alpha j\beta\ell'}^{\ell} &= -\frac{q M_{\alpha\beta,\ell\ell'}}{12\nu_{k_\ell}} \Big(\frac{q\mu_0}{3} + (-1)^{\alpha+j+1}\frac{k_\ell}{\sqrt{6}} - (-1)^{\beta+j+1}\frac{k_{\ell'}}{\sqrt{6}} \Big) v_{-\beta j}^{(0,\ell')}.
\end{aligned}
\tag{A.5}
$$

- The coefficients in (4.44)

$$
\begin{aligned}
\mathtt{s}_{1\alpha j\ell'}^{\ell} &= \int_\infty^\varepsilon dz \frac{\eta_1 F(z)}{c_{\alpha j}^{\ell} z^2 h_{\alpha j}} + \frac{q}{6c_{\alpha j}^{\ell}} \sum_\beta M_{\alpha\beta,\ell\ell'} \Big[\ln\varepsilon D_{1\beta} + \varepsilon^{-2\nu_{k_\ell}} (-\frac{D_{2\beta}}{2\nu_{k_\ell}} - \frac{D_{4\beta}}{4\nu_{k_\ell}^2})\\
&\quad + \frac{(\ln\varepsilon)^2}{2} D_{3\beta} - \frac{1}{2\nu_{k_\ell}} \epsilon^{-2\nu_{k_\ell}} \ln\varepsilon D_{4\beta} + (\frac{D_{1\beta}}{2\nu_{k_\ell}} - \frac{D_{3\beta}}{4\nu_{k_\ell}^2}) \Big];\\
\mathtt{s}_{2\alpha j\ell'}^{\ell} &= -\int_\infty^\varepsilon dz \frac{\eta_2 F(z)}{c_{\alpha j}^{\ell} z^2 h_{\alpha j}} - \frac{q}{6c_{\alpha j}^{\ell}} \sum_\beta M_{\alpha\beta,\ell\ell'} \Big[\ln\varepsilon D_{2\beta} + \varepsilon^{2\nu_{k_\ell}} (\frac{D_{1\beta}}{2\nu_{k_\ell}} - \frac{D_{3\beta}}{4\nu_{k_\ell}^2})\\
&\quad + \frac{(\ln\varepsilon)^2}{2} D_{4\beta} + \frac{1}{2\nu_{k_\ell}} \epsilon^{-2\nu_{k_\ell}} \ln\varepsilon D_{3\beta} + (-\frac{D_{2\beta}}{2\nu_{k_\ell}} - \frac{D_{4\beta}}{4\nu_{k_\ell}^2}) \Big];
\end{aligned}
$$

$$\mathrm{s3}^{\ell}_{\alpha j\ell'} = \int_{\infty}^{\varepsilon} dz \frac{\eta_1 G(z)}{c^{\ell}_{\alpha j} z^2 h_{\alpha j}} + \frac{q}{6c^{\ell}_{\alpha j}} \sum_{\beta} M_{\alpha\beta,\ell\ell'} \Big[(\ln\varepsilon + \frac{1}{\nu_{k_\ell}}) D_{3\beta} + \varepsilon^{-2\nu_{k_\ell}} \frac{D_{4\beta}}{2\nu_{k_\ell}} - D_{1\beta} \Big];$$

$$\mathrm{s4}^{\ell}_{\alpha j\ell'} = -\int_{\infty}^{\varepsilon} dz \frac{\eta_2 G(z)}{c^{\ell}_{\alpha j} z^2 h_{\alpha j}} - \frac{q}{6c^{\ell}_{\alpha j}} \sum_{\beta} M_{\alpha\beta,\ell\ell'} \Big[-\ln\varepsilon D_{4\beta} + \varepsilon^{2\nu_{k_\ell}} \frac{D_{3\beta}}{2\nu_{k_\ell}} - D_{2\beta} \Big];$$

$$\mathrm{s5}^{\ell}_{\alpha j\ell'} = -\frac{q}{6c^{\ell}_{\alpha j}} \sum_{\beta} M_{\alpha\beta,\ell\ell'} \Big[D_{1\beta} - \frac{D_{3\beta}}{2\nu_{k_\ell}} \Big];$$

$$\mathrm{s6}^{\ell}_{\alpha j\ell'} = -\frac{q}{6c^{\ell}_{\alpha j}} \sum_{\beta} M_{\alpha\beta,\ell\ell'} \Big[-D_{2\beta} - \frac{D_{4\beta}}{2\nu_{k_\ell}} \Big];$$

$$\mathrm{s7}^{\ell}_{\alpha j\ell'} = -\frac{q}{6c^{\ell}_{\alpha j}} \sum_{\beta} M_{\alpha\beta,\ell\ell'} 2D_{3\beta};$$

$$\mathrm{s8}^{\ell}_{\alpha j\ell'} = -\frac{q}{6c^{\ell}_{\alpha j}} \sum_{\beta} M_{\alpha\beta,\ell\ell'} \Big[\frac{3}{2} D_{3\beta} \Big];$$

$$\mathrm{s9}^{\ell}_{\alpha j\ell'} = -\frac{q}{6c^{\ell}_{\alpha j}} \sum_{\beta} M_{\alpha\beta,\ell\ell'} \Big[\frac{1}{2} D_{4\beta} \Big];$$

$$\mathrm{s10}^{\ell}_{\alpha j\ell'} = -\frac{q}{6c^{\ell}_{\alpha j}} \sum_{\beta} M_{\alpha\beta,\ell\ell'} \Big[\frac{1}{2} D_{3\beta} \Big];$$

$$\mathrm{s11}^{\ell}_{\alpha j\ell'} = \frac{q}{6c^{\ell}_{\alpha j}} \sum_{\beta} M_{\alpha\beta,\ell\ell'} \Big[\frac{1}{2} D_{4\beta} \Big]$$

with

$$\begin{aligned}
D_{1\beta} &= \tilde{d}1^{\ell'}_{\beta j,\alpha\ell} - \frac{(-1)^j \nu_{k_{\ell'}}}{\frac{q\mu_0}{6} + (-1)^{\alpha+j+1}\frac{k_\ell}{\sqrt{6}}} \tilde{d}1^{\ell'}_{\beta l,\alpha\ell} + d3^{\ell'}_{\beta l,\alpha\ell}; \\
D_{2\beta} &= d4^{\ell'}_{\beta l,\alpha\ell}; \\
D_{3\beta} &= d3^{\ell'}_{\beta j,\alpha\ell} - \frac{(-1)^j \nu_{k_{\ell'}}}{\frac{q\mu_0}{6} + (-1)^{\alpha+j+1}\frac{k_\ell}{\sqrt{6}}} d3^{\ell'}_{\beta l,\alpha\ell}; \\
D_{4\beta} &= d4^{\ell'}_{\beta j,\alpha\ell} - \frac{(-1)^j \nu_{k_{\ell'}}}{\frac{q\mu_0}{6} + (-1)^{\alpha+j+1}\frac{k_\ell}{\sqrt{6}}} d4^{\ell'}_{\beta l,\alpha\ell}.
\end{aligned} \tag{A.6}$$

- The coefficients in (5.11)

  Note that near $\omega = 0, k = k_F$, we expand

$$\begin{aligned}
&A^{(0)-}_{\alpha\ell,\alpha\ell} v^{(0,\ell)}_{-\alpha 2} + \epsilon^2 A^{(2,5)}_{\alpha\ell} \tilde{s}5^{\ell}_{\alpha 2} - \epsilon^2 \sum_{\beta,\ell'=\ell\pm 1} \frac{A^{(1,4)}_{\beta\ell',\alpha\ell} n4^{\ell'}_{\beta 2\alpha\ell} A^{(1,4)}_{\alpha\ell,\beta\ell'} n4^{\ell}_{\alpha 2\beta\ell'}}{A^{(0)-}_{\beta\ell',\beta\ell'} v^{(0,\ell')}_{-\beta 2}} \\
&= e_1\omega - e_2(k_\ell - k_F) + \ldots
\end{aligned} \tag{A.7}$$

where in the above formulae, we have substituted $A^{\rm UV} = A^{(0)} + \omega A^{(1)} + ...$

$$Ze_1 = B^{(0)-}_{\alpha\ell,\alpha\ell} v^{(0,\ell)}_{-\alpha 1}; \tag{A.8}$$

$$v_F e_1 = e_2; \tag{A.9}$$

$$\alpha_{\vec{k}} e_1 = A^{(0)+}_{\alpha\ell,\alpha\ell} v^{(0,\ell)}_{+\alpha 2} \tilde{\mathcal{G}}^{\ell}_{\alpha} + \epsilon^2 \Bigg(A^{(2,1)}_{\alpha\ell} \tilde{s_1}^{\ell}_{\alpha 2} + A^{(2,4)}_{\alpha\ell} {s_4}^{\ell}_{\alpha 2} - \sum_{\beta\ell'=\ell\pm 1} \frac{A^{(1,4)}_{\alpha\ell,\beta\ell'} {n_4}^{\ell}_{\alpha 2\beta\ell'} A^{(1,3)}_{\alpha\ell',\beta\ell} {n_3}^{\ell'}_{\alpha 2\beta\ell}}{A^{(0)-}_{\alpha\ell',\alpha\ell'} v^{(0,\ell')}_{-\alpha 2}} \Bigg) \tag{A.10}$$

$$\beta^{(1)}_{\vec{k}} e_1 = -\epsilon^2 \sum_{\beta\ell'=\ell-1} \frac{A^{(1,3)}_{\alpha\ell,\beta\ell'} {n_3}^{\ell}_{\alpha 2\beta\ell'} A^{(1,4)}_{\alpha\ell',\beta\ell} {n_4}^{\ell'}_{\alpha 2\beta\ell}}{A^{(0)-}_{\alpha\ell',\alpha\ell'} v^{(0,\ell')}_{-\alpha 2}}; \tag{A.11}$$

$$\beta^{(2)}_{\vec{k}} e_1 = \epsilon^2 A^{(2,3)}_{\alpha\ell,\ell-1} {s_3}^{\ell}_{\alpha 2\ell-1} - \epsilon^2 \sum_{\beta\ell'=\ell-1} \frac{A^{(1,1)}_{\alpha\ell,\beta\ell'} \tilde{n_1}^{\ell}_{\alpha 2\beta\ell'} A^{(1,4)}_{\alpha\ell',\beta\ell} {n_4}^{\ell'}_{\alpha 2\beta\ell}}{A^{(0)-}_{\alpha\ell',\alpha\ell'} v^{(0,\ell')}_{-\alpha 2}} - \epsilon^2 \sum_{\beta\ell'=\ell-1} \frac{A^{(1,4)}_{\alpha\ell,\beta\ell'} {n_4}^{\ell}_{\alpha 2\beta\ell'} A^{(1,1)}_{\alpha\ell',\beta\ell} \tilde{n_1}^{\ell'}_{\alpha 2\beta\ell}}{A^{(0)-}_{\alpha\ell',\alpha\ell'} v^{(0,\ell')}_{-\alpha 2}}; \tag{A.12}$$

$$\beta^{(3)}_{\vec{k}} e_1 = \epsilon^2 \tilde{A}^{(2,4)}_{\alpha\ell} \tilde{s}^{\ell}_{4\alpha 2}; \tag{A.13}$$

$$\beta^{(4)}_{\vec{k}} e_1 = \epsilon^2 A^{(2,3)}_{\alpha\ell,\ell+1} {s_3}^{\ell}_{\alpha 2\ell+1} - \epsilon^2 \sum_{\beta\ell'=\ell+1} \frac{A^{(1,1)}_{\alpha\ell,\beta\ell'} \tilde{n_1}^{\ell}_{\alpha 2\beta\ell'} A^{(1,4)}_{\alpha\ell',\beta\ell} {n_4}^{\ell'}_{\alpha 2\beta\ell}}{A^{(0)-}_{\alpha\ell',\alpha\ell'} v^{(0,\ell')}_{-\alpha 2}} - \epsilon^2 \sum_{\beta\ell'=\ell+1} \frac{A^{(1,4)}_{\alpha\ell,\beta\ell'} {n_4}^{\ell}_{\alpha 2\beta\ell'} A^{(1,1)}_{\alpha\ell',\beta\ell} \tilde{n_1}^{\ell'}_{\alpha 2\beta\ell}}{A^{(0)-}_{\alpha\ell',\alpha\ell'} v^{(0,\ell')}_{-\alpha 2}}; \tag{A.14}$$

$$\beta^{(5)}_{\vec{k}} e_1 = -\epsilon^2 \sum_{\beta\ell'=\ell+1} \frac{A^{(1,3)}_{\alpha\ell,\beta\ell'} {n_3}^{\ell}_{\alpha 2\beta\ell'} A^{(1,4)}_{\alpha\ell',\beta\ell} {n_4}^{\ell'}_{\alpha 2\beta\ell}}{A^{(0)-}_{\alpha\ell',\alpha\ell'} v^{(0,\ell')}_{-\alpha 2}}. \tag{A.15}$$

References

[1] S. -S. Lee, "A Non-Fermi Liquid from a Charged Black Hole: A Critical Fermi Ball," Phys. Rev. D **79**, 086006 (2009) [arXiv:0809.3402 [hep-th]].

[2] H. Liu, J. McGreevy and D. Vegh, "Non-Fermi liquids from holography," Phys. Rev. D **83**, 065029 (2011) [arXiv:0903.2477 [hep-th]].

[3] M. Cubrovic, J. Zaanen and K. Schalm, "String Theory, Quantum Phase Transitions and the Emergent Fermi-Liquid," Science **325**, 439 (2009) [arXiv:0904.1993 [hep-th]].

[4] T. Faulkner, H. Liu, J. McGreevy and D. Vegh, "Emergent quantum criticality, Fermi surfaces, and AdS2," Phys. Rev. D **83**, 125002 (2011) [arXiv:0907.2694 [hep-th]].

[5] R. H. He et. al. "From a Single-Band Metal to a High-Temperature Superconductor via Two Thermal Phase Transitions", Science **331**, 1579 (2011) and refs therein. [arXiv:arXiv:1103.2329 [cond-mat]], [arXiv:arXiv:1103.2363 [cond-mat]] .

[6] Y. Kohsaka et. al. "How Cooper pairs vanish approaching the Mott insulator in $Bi_2Sr_2CaCu_2O_{8+\delta}$", Nature **454** 1072 (2008) and refs therein. [arXiv:0808.3816 [cond-mat]].

[7] N. Mannella et al. "Nodal quasiparticle in pseudogapped colossal magnetoresistive manganites", Nature **438**, 474 (2005) [arXiv:cond-mat/0510423].

[8] H. M. Ronnow et al. "Polarons and confinement of electronic motion to two dimensions in a layered transition metal oxide", Nature **440**, 1025 (2006) [arXiv:cond-mat/0511138].

[9] F. Massee at al. "Bilayer manganites: polarons in the midst of a metallic breakdown", Nature Physics **7**, 978 (2011) [arXiv:1103.3804 [cond-mat]].

[10] J. P. Gauntlett, J. Sonner and D. Waldram, "Universal fermionic spectral functions from string theory," Phys. Rev. Lett. **107**, 241601 (2011) [arXiv:1106.4694 [hep-th]].

[11] R. Belliard, S. S. Gubser and A. Yarom, "Absence of a Fermi surface in classical minimal four-dimensional gauged supergravity," JHEP **1110**, 055 (2011) [arXiv:1106.6030 [hep-th]].

[12] J. Gauntlett, J. Sonner and D. Waldram, "Spectral function of the supersymmetry current," JHEP **1111**, 153 (2011) [arXiv:1108.1205 [hep-th]].

[13] T. Faulkner and J. Polchinski, "Semi-Holographic Fermi Liquids," JHEP **1106**, 012 (2011) [arXiv:1001.5049 [hep-th]].

[14] S. A. Hartnoll, J. Polchinski, E. Silverstein and D. Tong, "Towards strange metallic holography," JHEP **1004**, 120 (2010) [arXiv:0912.1061 [hep-th]].

[15] S. A. Hartnoll and A. Tavanfar, "Electron stars for holographic metallic criticality," Phys. Rev. D **83**, 046003 (2011) [arXiv:1008.2828 [hep-th]].

[16] M. Cubrovic, J. Zaanen and K. Schalm, "Constructing the AdS Dual of a Fermi Liquid: AdS Black Holes with Dirac Hair," JHEP **1110**, 017 (2011) [arXiv:1012.5681 [hep-th]].

[17] M. Cubrovic, Y. Liu, K. Schalm, Y. -W. Sun and J. Zaanen, "Spectral probes of the holographic Fermi groundstate: dialing between the electron star and AdS Dirac hair," Phys. Rev. D **84**, 086002 (2011) [arXiv:1106.1798 [hep-th]].

[18] S. Sachdev, "A model of a Fermi liquid using gauge-gravity duality," Phys. Rev. D **84**, 066009 (2011) [arXiv:1107.5321 [hep-th]].

[19] A. Allais, J. McGreevy and S. J. Suh, "A quantum electron star," arXiv:1202.5308 [hep-th].

[20] S. A. Hartnoll and D. M. Hofman, "Locally critical umklapp scattering and holography," arXiv:1201.3917 [hep-th].

[21] G. T. Horowitz, J. E. Santos and D. Tong, "Optical Conductivity with Holographic Lattices," arXiv:1204.0519 [hep-th].

[22] A. Aperis, P. Kotetes, E. Papantonopoulos, G. Siopsis, P. Skamagoulis and G. Varelogiannis, "Holographic Charge Density Waves," Phys. Lett. B **702**, 181 (2011) [arXiv:1009.6179 [hep-th]].

[23] R. Flauger, E. Pajer and S. Papanikolaou, "A Striped Holographic Superconductor," Phys. Rev. D **83**, 064009 (2011) [arXiv:1010.1775 [hep-th]].

[24] V. Keranen, E. Keski-Vakkuri, S. Nowling and K. P. Yogendran, "Inhomogeneous Structures in Holographic Superfluids: I. Dark Solitons," Phys. Rev. D **81**, 126011 (2010) [arXiv:0911.1866 [hep-th]].

[25] G. T. Horowitz, J. E. Santos and B. Way, "A Holographic Josephson Junction," Phys. Rev. Lett. **106**, 221601 (2011) [arXiv:1101.3326 [hep-th]].

[26] K. Maeda, T. Okamura and J. i. Koga, "Inhomogeneous charged black hole solutions in asymptotically anti-de Sitter spacetime," arXiv:1107.3677 [gr-qc].

[27] J. A. Hutasoit, S. Ganguli, G. Siopsis and J. Therrien, "Strongly Coupled Striped Superconductor with Large Modulation," JHEP **1202**, 086 (2012) [arXiv:1110.4632 [cond-mat.str-el]].

[28] A. M. Garcia-Garcia, J. E. Santos and B. Way, "Holographic Description of Finite Size Effects in Strongly Coupled Superconductors," arXiv:1204.4189 [hep-th].

[29] S. Ganguli, J. A. Hutasoit and G. Siopsis, "Enhancement of Critical Temperature of a Striped Holographic Superconductor," arXiv:1205.3107 [hep-th].

[30] S. Kachru, A. Karch and S. Yaida, "Holographic Lattices, Dimers, and Glasses," Phys. Rev. D **81**, 026007 (2010) [arXiv:0909.2639 [hep-th]].

[31] S. Bolognesi and D. Tong, "Monopoles and Holography," JHEP **1101**, 153 (2011) [arXiv:1010.4178 [hep-th]].

[32] N. Iqbal, H. Liu and M. Mezei, "Semi-local quantum liquids," arXiv:1105.4621 [hep-th].

[33] T. Faulkner, N. Iqbal, H. Liu, J. McGreevy and D. Vegh, "Strange metal transport realized by gauge/gravity duality," Science **329**, 1043 (2010).

[34] H. Takagi et.al. "Systematic Evolution of Temperature-dependent Resistivity in $La_{2-x}Sr_xCuO_4$", Phys. Rev. Lett. **69**, 2975 (1992).

[35] J. M. Tranquada et.al. "Evidence for unusual superconducting correlations coexisting with stripe order in La(1.875)Ba(0.125)CuO(4)", Phys. Rev. B **78**, 174529 (2008) [arXiv:0809.0711 [cond-mat]].

[36] e.g. Y. Tokura, "Critical features of colossal magnetoresistive manganites", Rep. Prog. Phys. **69**, 797 (2006) and refs therein.

[37] T. Faulkner, N. Iqbal, H. Liu, J. McGreevy, D. Vegh, "Holographic non-Fermi liquid fixed points," [arXiv:1101.0597 [hep-th]].

[38] T. Faulkner, G. T. Horowitz, J. McGreevy, M. M. Roberts and D. Vegh, "Photoemission 'experiments' on holographic superconductors," JHEP **1003**, 121 (2010) [arXiv:0911.3402 [hep-th]].

[39] V. Alexandrov and P. Coleman, "Spin and holographic metals," [arXiv:1204.6310[cond-mat]]

[40] C. P. Herzog and J. Ren, "The Spin of Holographic Electrons at Nonzero Density and Temperature," JHEP **1206**, 078 (2012) [arXiv:1204.0518 [hep-th]].

[41] S. S. Gubser, F. D. Rocha and P. Talavera, "Normalizable fermion modes in a holographic superconductor," JHEP **1010**, 087 (2010) [arXiv:0911.3632 [hep-th]].

[42] D. Vegh, "Fermi arcs from holography," arXiv:1007.0246 [hep-th].

[43] F. Benini, C. P. Herzog, R. Rahman and A. Yarom, "Gauge gravity duality for d-wave superconductors: prospects and challenges," JHEP **1011**, 137 (2010) [arXiv:1007.1981 [hep-th]].

[44] S. Nakamura, H. Ooguri and C. -S. Park, "Gravity Dual of Spatially Modulated Phase," Phys. Rev. D **81**, 044018 (2010) [arXiv:0911.0679 [hep-th]].

[45] A. Donos and J. P. Gauntlett, "Holographic striped phases," JHEP **1108**, 140 (2011) [arXiv:1106.2004 [hep-th]].

[46] O. Bergman, N. Jokela, G. Lifschytz and M. Lippert, "Striped instability of a holographic Fermi-like liquid," JHEP **1110**, 034 (2011) [arXiv:1106.3883 [hep-th]].

[47] S. Kachru, A. Karch and S. Yaida, "Adventures in Holographic Dimer Models," New J. Phys. **13**, 035004 (2011) [arXiv:1009.3268 [hep-th]].